Addis Ababa Institute Of Technology

Center For Ethio-Mines Development

Master of Engineering in Mineral Engineering

Mineralogical Characterization and Comminution Energy Requirement of Lithium-Bearing Pegmatite in Burkuke, Sidama Regional State, Ethiopia

By Deneke Gizaw

A Project submitted to the center for Ethio-mines development, Addis Ababa Institute of technology, Addis Ababa university in the Partial fulfillment of the requirements for the Degree of Master of Engineering in Mineral Engineering

Advisor: Kebede Gamo (Ph.D)

Date: May, 2025

Addis Ababa University, Ethiopia

Approval Sheet

This is to certify that the research project prepared by **Deneke Gizaw Mazenga** entitled: "**Mineralogical Characterization and Comminution Energy Requirement of Lithium-Bearing Pegmatite in Burkuke, Sidama Regional State, Ethiopia**" and submitted in partial fulfillment of the requirements for the degree of Master of Engineering in Mineral Engineering compiles with the regulations of the university and meets the accepted standards with respect to originality and quality.

Submitted by: Deneke Gizaw **Signature** _____ **Date** 02/06/2025

Approved by:

Name	Signature	Date
Advisor: Dr. Kebede Gamo	_____	02/06/2025
External Examiner: Dr. Bekele Ayele	_____	02/06/2025
Internal Examiner: Dr. Zekarias Gebreyes	_____	02/06/2025

Authorship Declaration

I hereby to declare that the project "**Mineralogical Characterization and Comminution Energy Requirement of Lithium-Bearing Pegmatite in Burkuke, Sidama regional state, Ethiopia**" has been carried out by the under the supervision of Kebede Gamo (Ph.D), Center for Ethio-Mines Development, Addis Ababa University, Addis Ababa Institute of technology in the year 2025 as a part of Master program in Mineral Engineering. I further declare that this project has not been submitted to any other university or institution anywhere for the award of any degree.

Author: Deneke Gizaw

Adress: Addis Ababa University

Date of submission: 03/06/2025

Signature: 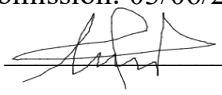

Acknowledgment

First and foremost, I would like to thank the merciful and Almighty God, for all the things done for me in my entire life. My deepest appreciation and sincere heartfelt gratitude go to my advisor Kebede Gamo (PhD) for his skillful assistance and devotion of his time in correcting and shaping the draft of this paper, continuing encouragement and all-round support throughout the research project.

Finally, I would like to thank the Center of Ethio-mines development, EFDR Ministry of mines and Addis Ababa institute of technology, Addis Ababa university and Sidama regional state mines and Energy agency and all others who provided me more valuable information and data to be successful in my research project.

Abstract

This study focuses on the mineralogical characterization and comminution energy requirement of lithium-bearing pegmatite located in the Burkuke locality in Sidama Regional state, Ethiopia. The increasing request of lithium around the world, used especially for batteries and renewable energy technologies, requires a deeper knowledge of mineralogical and chemical characteristics of pegmatites that is fundamental to develop the most efficient extraction techniques. The X-ray diffraction (XRD) analysis indicates that all three samples consist of multiple mineral phases and their compositions and abundances of minerals are different between the samples. XRD analysis confirmed the presence of critical lithium-bearing minerals Spodumene Present in all three samples (DE01: 30.1%, DE02: 10.3%, DE03: 12.6%), indicating moderate to significant lithium potential. Associated gangue minerals: Quartz, feldspar, albite, muscovite, and biotite, which can affect the liberation and separation processes. According to the results of the Atomic absorption spectroscopy (AAS) analysis the content of lithium oxide in the concentrates is relatively low (0.09%) and this is an integral factor in taking into account of the possibility of lithium extraction from this pegmatite. The findings indicate that although fine grinding enhances mineral liberation, energy consumption requires particular attention when processing operations are performed on an industrial scale. From grinding data, it is found that the feed size, the milling speed, and the amount of consumed energy affect the size reduction phenomenon. Sample 1 (350 rpm, 3.35 kWh/ton, P80 320 μm), Sample 2 (700 rpm, 5.01 kWh/ton, P80 200 μm), Sample 3 (1050 rpm,1.53 kWh/ton, P80 620 μm), and Sample 4 (3.365 kWh/ton, P80 1.3 mm).

Keywords: Characterization, comminution, energy, lithium, mineralogy

Table of contents

List of Tables

List of Figures

List of Acronyms

AAS ---------- Atomic Absorption Spectroscopy

EVs ---------- Electric Vehicles

LCT ---------- Lithium-cesium-tantalum family

Ppm ---------- Parts per million

REE ---------- Rare earth elements

RPM --------- Revolution per minute

OFTB ------- Ophiolitic Fold and Thrust Belt

MLA -------- Mineral Liberation Analysis

XRD -------- X-ray Diffraction

XRF --------- X-ray fluorescence

LOI ---------- Loss On Ignition

1. Introduction

1.1. Background

Lithium has received a lot of attention owing to its use in batteries and other technological sectors. A central source of lithium, pegmatites need to be studied in terms of their properties for extraction and processing to be efficient. Pegmatites are famous for their economically important minerals and large crystal size, lithium-bearing varieties like spodumene and lepidolite are no exception (Dharmapriya et al., 2025). Characterization of these pegmatite is important for assessing their mining and processing (Rajhi et al., 2024). Ethiopia, in turn, seeks to make effective use of its mineral resources which has sustainable developments while considering environmental impacts. With rich geological structures, Ethiopia has a good number of lithium-bearing pegmatites (Küster et al,. 2009). The processing of lithium from spodumene entails a number of processing steps, comminution being the one. Comminution aids in the liberation of spodumene crystals by reducing their size which makes them ready for the next stages of processing (Whitworth et al., 2022). In order to provide information on its development as a resource, this research aims to study the petrographic and chemical characterization of lithium-bearing pegmatite in the Burkuke area of Chabe Woreda in Sidama Region.

1.1.1. Regional Geology and African Pegmatite Mineralization

The Precambrian basement rocks of Africa are noted for containing important deposits of pegmatitic minerals, especially where there are traces of Pan-African orogeny and cratonic regions. Some African countries such as Zimbabwe, Namibia, Mali and the Democratic Republic of Congo have documented occurrences of lithium pegmatites. In Zimbabwe, the Bikita deposit is regarded as one of the largest and oldest exploited sustenance of lithium owing to the spodumene and petalite hosted within complex zoned pegmatites (Bradley et al., 2017). Likewise, Uis pegmatites in Namibia that were mined for tin are being re-assessed for their lithium content owing to lepidolite and petalite (Bleiwas, 2018).

1.1.2. Geology of Ethiopia and Pegmatite Potential

The Ethiopian geological setting consisting of the neoproterozoic basement complexes of the Arabian-Nubian Shield and Mozambique Belt offers an ideal setting for the development of pegmatites (Stern et al., 2012). These belts contain highly metamorphosed terrains with granitic and pegmatitic intrusions which are commonly depleted in industrial minerals and rare metals. The Southern Ethiopian Shield including the Adola belt and its vicinity is known to host extensive pegmatitic intrusions, some of which contain lithium bearing minerals (Stern et al.,

2012). (Stern et al., 2012) cited some pegmatites with spodumene, beryl, and muscovite which indicates that some of these deposits might be economically viable. Although there are encouraging signs, the lack of detailed geochemical and processing investigations indicates a gap in the country's exploration and beneficiation plans. Lithium as well as other critical minerals have recently become the center of attention for some government and foreign investors regarding the Homegrown Economic Reforms Agenda. The Ministry of Mines (2023) reports that geological surveys have located lithium pegmatites in the Oromiya, SNNPR, and Sidama regional states, but are still in the nascent stages of exploration.

1.2. Statement of the Problem

Even with the growing worldwide need for lithium, Ethiopia's lithium bearing pegmatites remain under researched for their characterization and energy efficient processing. The lack of detailed mineralogical information regarding the pegmatites in the Burkuke coupled with insufficient understanding of effective comminution processes for lithium extraction presents a gap which lack of detail exploration of the country economic feasibility of lithium extraction. Additionally, a lack of adequate information regarding their mineralogical characteristics and effective comminution techniques prevents the formulation of strategies for responsible mining and the use of inefficient practices results in low recovery rates which undermines the potential value of local lithium resources. In the absence of effective characterization and processing frameworks, the possible economic value of lithium extraction in the country is likely to remain unexploited.

1.3. Objectives of the Study

Mineralogical characterization and comminution energy requirement of lithium-bearing pegmatite in Burkuke area Sidama Regional State, Ethiopia .

1.3.1. Specific objectives

1. To characterize the mineralogical composition of lithium-bearing pegmatite in the study area.
2. To evaluate the effectiveness of various comminution techniques on lithium recovery.
3. To analyze the impact of particle size on lithium liberation.
4. To analyze the distribution of lithium and associated elements within the pegmatite samples.
5. To recommend optimal processing conditions for maximizing lithium extraction and for sustainable mining practices.

1.4. Significance of the study

The study on the characterization and comminution of lithium-bearing pegmatites from the Burkuke deposit in Sidama Regional state, Ethiopia holds significant importance as it confirms the presence of economically valuable minerals like spodumene and rare earth elements, which are critical for renewable energy and high-tech industries. This study seeks to improve sustainable mining approaches and recovery rates while aiding Ethiopia's entry into the global lithium market, which would enhance the economy as well as technological advancements, by optimizing the comminution processes and assessing lithium content.

1.5. Scope of the Study

The study focuses on the Burkuke locality within Sidama regional state, examining local pegmatite formations for lithium content and suitability for extraction. The research will cover mineralogical analysis, and comminution process evaluations.

1. Geological sampling, mineralogical analysis, and comminution testing.
2. Analysis of crushing and grinding methods, including jaw crushers and ball mills.
3. Measurement and comparison of energy consumption for different comminution methods.
4. Statistical analysis of experimental data to develop optimized comminution strategies.
5. Proposing optimization strategies for lithium recovery in the study area.

1.6. Description and Accessibility of the Study Area

The study area isfrom Addis Ababa to Hawassa 275 km along asphalt. Again, from Hawassa to Bensa asphalt distance 140 km. however, the road from Bensa to Chabe Ganbeltu. The road from Bensa to Chabe Ganbeltu, which is nearer to the study area, is surfaced. These roads are surfaced and accessible by vehicle during the dry season.

Location map of study area

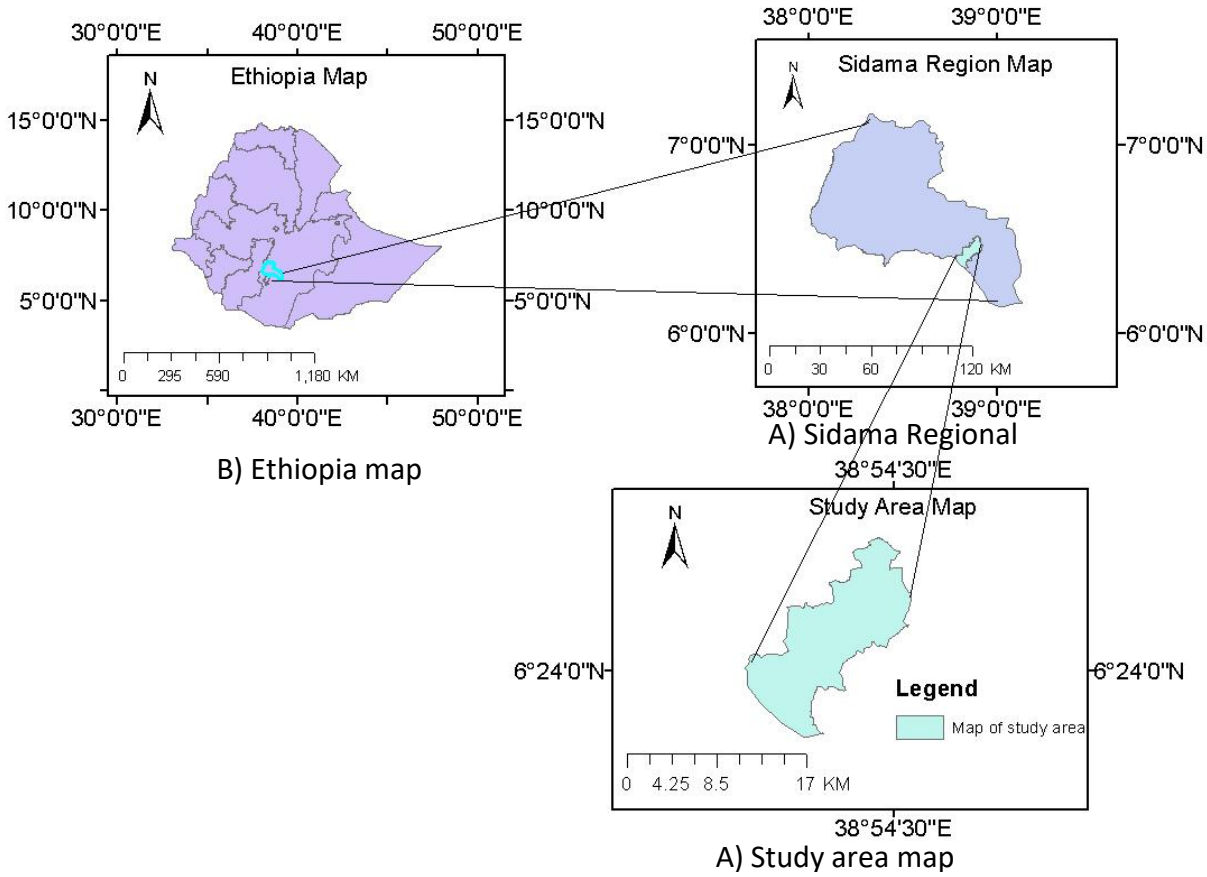

Figure 1.1 Location map of study area

2. Literature Review

2.1. Introduction

Demand for lithium has notably surged in the last few years owing to the increasing use of rechargeable batteries in lithium-powered portable electronics like mobile phones, computers, and electric power tools, in addition to electric cars (Asmare et al., 2024). Spodumene (6.0 – 7.5% Li_2O) in high-grade lithium-caesium-tantalum (LCT) pegmatite deposits is a major source of lithium. Other lithium minerals of commercial value include petalite (3.5–4.5% Li_2O) and Li-bearing micas (polylithionite, trilithionite, lepidolite, and zinnwaldite), which contain Li_2O ranging from 2.0% to 7.7% (Maneta et al., 2015). Spodumene naturally occurs in the α-monoclinic (C2/c) form as a member of the pyroxene group and is commonly found associated with quartz, albite, microcline, and micas in pegmatite deposits (Gil-Alana & Monge, 2019). LCT pegmatites often contain high concentrations (> 0.9%) of rubidium and caesium, which can also be recovered as byproducts (Aylmore et al., 2018). Various processes have been developed to recover lithium from Li-bearing minerals, including spodumene. In terms of minerals, lithium is currently extracted predominantly from pegmatite deposits, with spodumene being the most important Li-bearing mineral, and petalite and lepidolite representing sources of minor economic importance (Balaram et al., 2024). Lithium is most commonly associated with Li-ion batteries that power modern mobile electronic devices, but it has a wide range of other applications.As stated by Zubi et al (2018), key drivers like the growth of population and the expansion of developing countries will have a considerable impact on the prospective need for lithium.

2.2. Pegmatite Field and Lithium deposits in Ethiopia

Geological Formation:

The northwestern section of the Neoproterozoic basement in southern Ethiopia is referred to as the Adola Belt, which comprises the Adola granite–gneiss complex (Küster et al., 2009). The geological history of these regions involves significant tectonic activity, granite intrusions, and subsequent hydrothermal processes, all of which contribute to the formation of these mineral-rich bodies (Tadesse, 2001). The tectonic events and granite intrusions in the Adola Terrain, in particular, have created favorable conditions for the formation of lithium-bearing pegmatites, which are enriched in minerals such as spodumene (Küster et al., 2009). The deposit has an estimated 250,000 tonnes of Li_2O, along with byproduct tantalum (Ta), niobium (Nb), and beryllium (Be) (Tadesse, 2001).

The metamorphic rocks of the Mozambique Orogenic Belt (MB) underlie the area of the study. The region also has some metamorphic rocks as well as granitic intrusives. (Mohammedyasin,

2017). Basalt forms the igneous rocks of the area together with granite and pegmatite intrusives. The macroscopic minerals of the area are mica (both biotite and muscovite), plagioclase feldspar, chlorite, quartz, and other accessory minerals. Ethiopia is richly diverse in geology, and this diversity makes the country a potential area for lithium bearing pegmatites (Goodenough et al., 2025). The pegmatitic fields of the country are mostly found from the South eastern parts of the country, specifically in Sidama régional state and Oromia régional states. These pegmatites are most of the time abundant in the mineral spodumene which is essential for lithium mining extraction.

Lithium deposits

It is believed that the Southern Ethiopian Pegmatites included in this study possess a great deal of lithium, since numerous pegmatitic bodies in this area show scope of lithium mineralization and its geological setting is favorable for lithium bearing minerals (Tadesse, 2001).

Economic Lithium Deposits: These types of economical lithium deposits are found in two main forms in nature: Granite-pegmatites – This type consists of the world's most important lithium deposit, which is found mainly in the form of spodumene, lepidolite and petalite (Tadesse, 2001)

2.3. Comminution Circuit for Li -Pegmatite

Comminution is a critical process in the extraction of lithium from pegmatitic ores, as it involves breaking down the ore into smaller particles to liberate valuable minerals such as spodumene. An efficient comminution circuit is essential for maximizing lithium recovery and optimizing overall processing performance (Kwade et al., 2023).

2.3.1. Factors Influencing the Effectiveness of Comminution in Processing Lithium-Bearing Pegmatite

The Comminution step is an important step in recovering lithium contained in pegmatite ores. Many aspects may affect the efficiency of comminution, and thus the efficiency of recovery of lithium minerals.

Ore Composition - The particular mineral composition of spodumites within the pegmatite together with gangue constituents also influence the methods of comminution and the effectiveness of liberation (Timich et al., 2023).

Target Particle Size - Different degrees of fragmentation and the associated fulfillment of conditions for effective liberation of lithium can be achieved at different sizes. Comminution techniques differ with respect to ore characteristics like hardness, brittleness, and even mineralogy. For instance, jaw crushers are efficient in primary size reduction, while cone crushers are more suitable for finer reduction of harder ores. The same goes with ball, rod, stirrer mills.

The selection of these mills depends on the particle size required and the type of gangue minerals present (Kapadia, 2018).

Operational Parameters: The optimization of comminution processes is greatly affected by various settings. These include spindle speed, feeding rate, grinding time, and others. For optimizing mineral liberation, spodumene has to be separated from the gangue minerals without overgrinding, which requires optimizing operational parameters (Semsari Parapari et al., 2020). Smaller feed sizes, on the other hand, can reduce energy consumption during grinding, improving overall efficiency, but may lead to higher fines production, which can affect recovery rates (Whitworth et al., 2022).

Energy Efficiency: The energy consumed during comminution is one of the most Important factors. Process efficiency lowers cost and minimizes impact to the environment. Optimization of Energy Input: The overall processing effectiveness can be enhanced by achieving the optimal energy output ratio through parameter changes.

Mineral Association: The relationship between spodumene and gangue minerals has an influence on liberation for comminution.

Reactivity of Minerals: Some other chemical changes during the work like oxidation and hydration make some changes in the spodumene and can affect the ease of recovery.

Temperature and Humidity: Operating conditions can impact the performance of comminution equipment as well as the nature and characteristic of the feed material.

Handling of By-Products: Effective treatment and control of wastes generated from the process of comminution can enhance the operational sustainability (Hajam et al., 2023).

Handling of By-Products: Efficient handling and management of waste materials produced during comminution can impact the overall sustainability and feasibility of the operation (Hajam et al., 2023).

2.3.2. Impact of particle size on lithium liberation

The recovery and liberation of lithium is influenced by a range of particle sizes. Some of the notable effects are: Loss Reduction: Optimal spodumene recovery usually takes place at a specific particle size threshold. Enclosing spodumene comes with larger particles, whereas smaller ones tend to improve recovery effectiveness with some difficulties encountered at later stages of processing (Nandihalli et al., 2024).

Effects on Processing Methods: Spodumene separation is better from the gangue when optimal flotation levels for particle size are attained. On the other hand, recovery rates can be impacted negatively by overly coarse material, while fine particles increase the likelihood of separation complications due to slime formation (Sagzhanov et al., 2025).

Participation Expense: Size reduction to the most effective for liberation is best achieved through intensive comminution. For financial viability, having a lower bound on the size reduction while maintaining energy expenditure is essential. Finer particles enhance area, improving chemical processes like leaching and flotation, resulting in better lithium extraction rates due to increased reactivity.

2.4. The Characterization of Lithium-Bearing Pegmatites

Mineralogical Analysis: Mineral identification is crucial, with key lithium-bearing minerals including spodumene, lepidolite, petalite, and amblygonite (Balaram et al., 2024). The complex mineralogy of lithium-bearing pegmatites presents challenges for processing. Technological advances in processing techniques and reagents may improve recovery rates and reduce costs (Petrakis et al., 2025). Characterizing lithium-bearing pegmatites is essential for understanding their potential for lithium extraction and developing effective mining and processing strategies. This characterization involves several key aspects, including mineralogical, chemical, and physical analyses.

1. Mineralogical Composition

Primary Minerals: The most significant lithium-bearing minerals found in pegmatites include spodumene, lepidolite, and petalite. Each of these minerals has distinct properties affecting lithium recovery (Tian-ming et al., 2023).

Gangue Minerals:

Understanding the gangue minerals (e.g., quartz, feldspar, mica) is crucial, as they can influence the processing techniques and lithium recovery efficiency (Petrakis et al., 2025).

Lithium-Bearing Minerals:

Associated Minerals

Quartz (SiO_2) is a common gangue mineral in pegmatites and is typically found alongside lithium-bearing minerals; quartz does not contain lithium; it can affect separation processes due to its hardness and abundance in pegmatites (Breasley et al., 2025).

Feldspar includes both orthoclase and plagioclase varieties and is commonly found in pegmatites . Feldspars can act as gangue minerals and can affect the behavior of lithium minerals during processing; they need to be separated from lithium-bearing minerals to optimize extraction (Petrakis et al., 2025). Mica can affect processing techniques, particularly in flotation and separation processes, due to its layered structure and chemical composition. Tantalite ($(Fe, Mn)(Ta, Nb)_2O_6$) and Columbite are tantalite and niobium-bearing minerals that can occur in lithium pegmatites (Montana Bureau of Mines and Geology & Van Rythoven, 2023). These

minerals add economic value to pegmatites, as tantalum is a critical mineral used in electronics and other high-tech industries.

2.5. Application of lithium

1. Batteries

Electric Vehicles(EVs) Lithium- ion batteries are pivotal for powering electric vehicles(EVs) due to their high energy viscosity and long lifetime (Şen et al., 2024).

2. Energy Storage Systems

Renewable Energy Storage: Lithium-ion batteries are used in energy storage systems to store electricity from renewable sources like solar and wind (Koech et al., 2024).

3. Aerospace and Defense

Lithium-based batteries are critical in aerospace applications, where lightweight and high-energy density solutions are essential for improving fuel efficiency and reducing operational costs (Marsh et al., 2001).

4. Pharmaceuticals

Lithium compounds, particularly lithium carbonate, are used to treat bipolar disorder and other mental health conditions (Machado-Vieira et al., 2009).

5. Grease and Lubricants

Lithium-based greases are used in industrial applications for their high temperature resistance, stability, and ability to maintain lubricating properties under extreme conditions (Stefan-Henningsen et al., 2025).

2.6. Lithium mining and processing impacts

Lithium mining and processing can deeply affect the environment and local communities, particularly in places such as Ethiopia. From an environmental standpoint, lithium extraction, especially from brines, requires a lot of water. This is a major problem in dry regions because the extraction of water would deplete local water resources, negatively impacting local communities as well as the ecosystems. Economically, large scale mining structures could lead to the displacement of entire communities which disposes of social order. Additionally, developments on or a few floors of indigenous land can raise debates concerning the violation of human rights due to conflict over culture infringement over the natives bypassing local custom. In response, Ethiopia is currently formulating policies and guidelines on responsible sourcing that seek to regulate lithium mining in the country to promote social and environmental wellbeing. This includes engaging local communities in the management as well as enforcing clean cut mining policies (Vera et al., 2023).

3. Methodology and Materials

3.1. Sampling and samples preparation

3.1.1. Sample collection

Samples were collected from the Burkuke pegmatite deposit, located in the Sidama Regional state, Ethiopia. A Four samples were collected and totally 5 kg of Lithium Ore minerals was Collected from the lithium-bearing pegmatite deposit and properly cleaned to remove soil and other contaminants. The samples were labeled and stored in plastic bag to prevent contamination or loss of material.

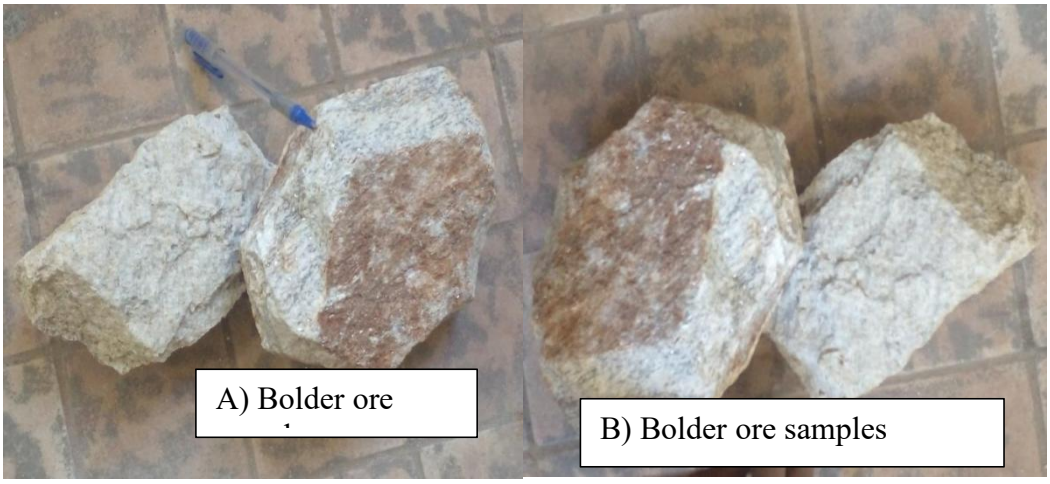

Figure 3.1 Lithium-bearing pegmatite bulk sample before comminution

3.1.2. Sample preparation

The initial sample, with an approximate size of 50 mm shown in (figure 3.2) below, was reduced using a jaw crusher followed by hammering to achieve a more manageable size. Perform crushing and collect the product. Sift the crushed material through a screen to ensure the material is reduced to desired size. Material larger than the set opening should be returned for additional crushing. Repeat the crushing process if necessary for larger portions until the entire 500 g sample is reduced to the desired size shown (Table 4.1) below. Ensure proper safety gear is worn, including goggles and gloves.

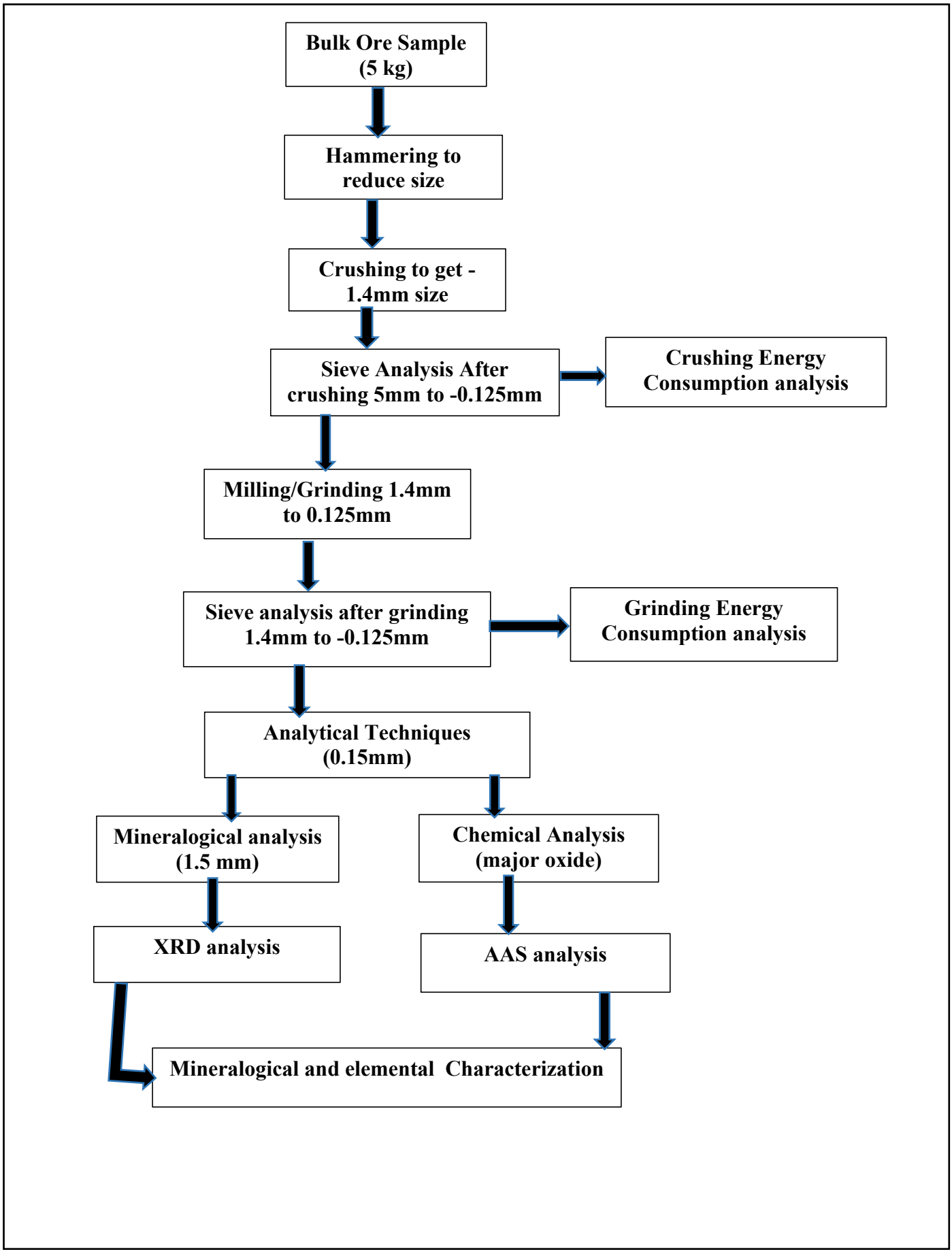
Bulk Ore Sample (5 kg)
Hammering to reduce size
Crushing to get -1.4mm size
Sieve Analysis After crushing 5mm to -0.125mm
Crushing Energy Consumption analysis
Milling/Grinding 1.4mm to 0.125mm
Sieve analysis after grinding 1.4mm to -0.125mm
Grinding Energy Consumption analysis
Analytical Techniques (0.15mm)
Mineralogical analysis (1.5 mm)
Chemical Analysis (major oxide)
XRD analysis
AAS analysis
Mineralogical and elemental Characterization

Figure 3.2 Lithium-bearing pegmatite samples after splitting by hammer

3.2. Comminution procedures

3.2.1. Crushing and Grinding processes

Crushing (Jaw Crusher)

Objective: Reduce sample size for further processing.

Equipment: Laboratory Jaw Crusher.

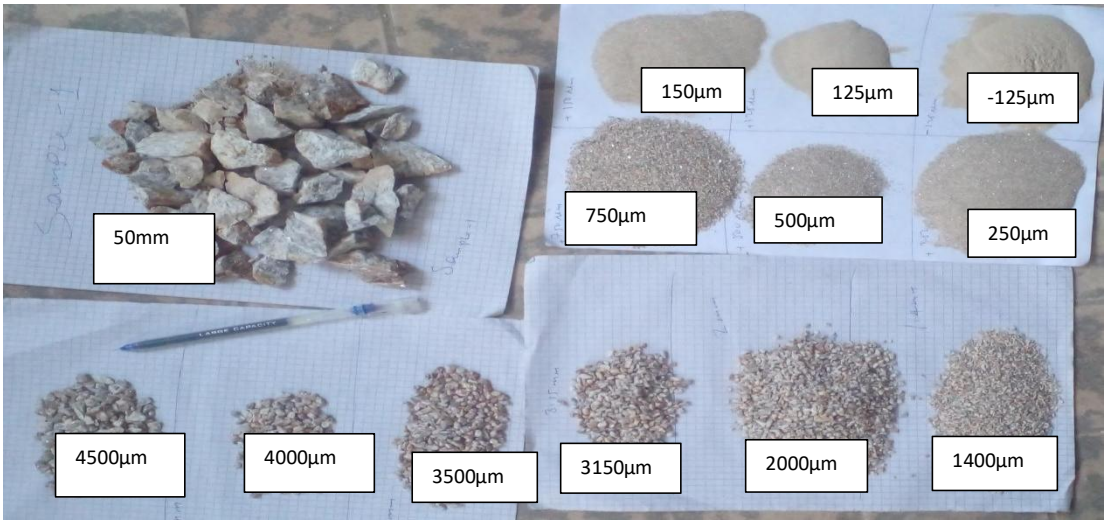

Figure 3.3 samples after comminution processes

Crushing Process:

Evaluating the various comminution techniques for lithium recovery from spodumine-bearing pegmatite is important for process optimization. The main comminution techniques and their effects on lithium recovery are:

Crushing: Jaw crushers are usually employed in the preliminary stages of size reduction, expertly converting large volumes of pegmatite into smaller rocks. Fine material production, which is important in the unlocking of spodumene from gangue minerals, is efficiently accomplished by impact crushers.

Grinding: Ball milling is widely employed for further size reduction which enhances the unlocking of spodumene. Rod milling has a similar approach, but is less efficient in liberation.

Jaw Crushing:

Jaw ddres the 5 g sample 50 mm sized granules using a jaw crusher. Collect and screen the resultant feeder material to the required screen grade. Any oversize is subjected to controlled crushing until the 500 g sample is at the required size stipulated in (Table 4.1). Subsequent to the first crushing step, a bulk portion of the material was divided into four 500 g portions for further processing.

Samples thinner than 0.01 g were weighted, followed by sieving.

Sieving Procedure:

Place the sample on the top sieve and run a mechanical shaker for 10 minutes at 60 mm amplitude (100 -200 oscillations per minute). The sieving indicated sizes between +4.5 mm and -0.125 mm, with a noticeable concentration in the finer size ranges. The samples were further quartered to proceed with the subsequent milling steps after sieving them.

Ball Milling:

Objective: Further reduce particle size for X-Ray Diffraction (XRD) and Atomic Absorption Spectroscopy (AAS) analysis, aiming for <0.15 mm in diameter.

Equipment and Conditions:

A laboratory ball mill with an internal diameter of 160 mm was used, with alumina balls of 21 mm and 27.1 mm. A total of four 250-gram samples with a maximum feed size of 1.4 mm were milled for 20 minutes in dry conditions at 350, 700, and 1050 rpm.

Details of Each Sample:

Sample 1: 350 rpm with a <2 mm feed; yielded 69 g that passed through a 0.15 mm sieve.

Sample 2: 700 rpm with identical feed; yielded 82 g that passed through a 0.15 mm sieve.

Sample 3: 1050 rpm with identical feed; yielded 93 g that passed through a 0.15 mm sieve.

Sample 4: 350 rpm and 2-4.5 mm feed; 74.7 g passed through a 0.15 mm sieve.

Monitoring:

To prevent excessive grinding, the progress of grinding was monitored.

Final Sieving and Sample Selection: After milling, the samples were subjected to a sieve analysis which lasted 10 minutes. Only the materials that were finer than 0.15 mm were kept for

XRD and AAS while everything else was discarded. For each sample, 0.5 g of the less than 0.15 mm fraction was extracted for analysis.

Grinding (Ball Mill) Parameters

Table 3.1 Grinding ball mill parameters

Items	Parameters		Value
Mill	Inner diameter (D) mm		160 mm
	Volume (V) cm^3		2,813,760 mm^3
	Length (L) mm		140 mm
Balls	Ball material		Alumina
	Ball diameter mm	Larger size	27.1 mm
		Smaller size	21 mm
	Number of balls	Larger size	20 balls
		Smaller size	40 balls
	Average ball weight g	Larger size ball	37.5 g each balls
		Smaller size ball	16.2 g each balls
	Total mass of balls		1398g
Feed material	Type		Spodumine
	Feed amount		Variable
	Feed size		1.4 mm and below
speed	Operational speed		350 rpm, 700 rpm, 1050 rpm

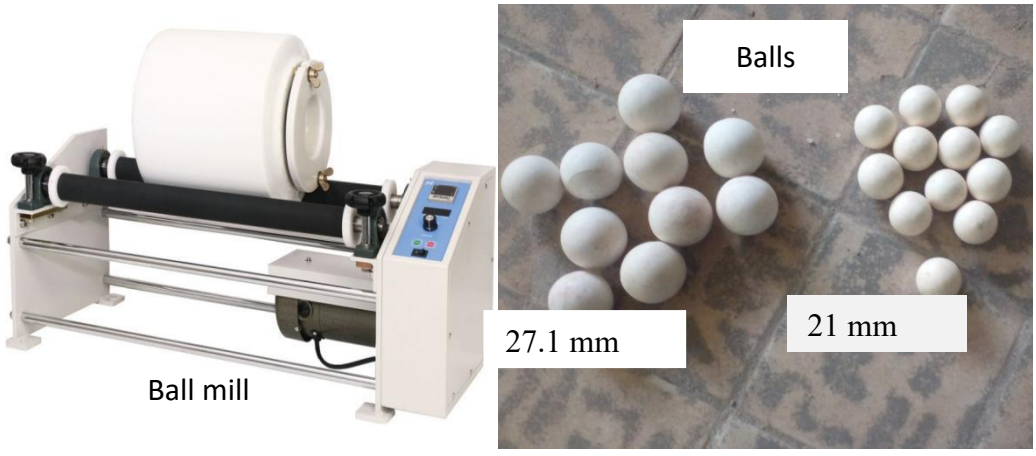

Figure 3.4 Grinder(Ball mill) and Balls

Analysis Preparation:

Prepared samples are suitable for X-ray diffraction and atomic absorption spectroscopy, ensuring accurate phase identification and mineralogical characterization of spodumene in the pegmatite.

X-ray Diffraction (XRD) Analysis

The three samples, sample codes (DE01, DE02, and DE03) were prepared by cleaning, splitting with a hammer, crushing, pulverizing, grinding, and sieving to a particle size of under 150 microns. A 0.5-gram sample from each batch was analyzed using X-ray diffraction (XRD). The analysis was conducted using latest version of Match4! and Origin pro softwares to identify the mineral phases present in each sample and Elemental analysis in each sample.

4. The Results, Discussion and Interpretations

4.1. Comminution Results

Crushing (Jaw Crusher)

Sample 1 had greater mass retention in the coarser fractions, and particularly on the +4.5 mm and +3.55 mm sieves, while Sample 2 showed greater concentration of finer particles with significant proportions in the +0.71 mm and pan (-0.125 mm) fractions. Both samples yielded the highest mass retention at the +2 mm sieve with Sample 1 jaw crushing giving 95.7 grams and Sample 2 yielding 102.4 grams suggesting mid-sized particles were dominant. Overall, sample 2 seemed to possess a finer distribution of particles as suggested by the greater retention in the smaller sieves and pan when compared to sample 1.

Sieve Size (mm)	Sample 1 Mass Retained (grams)	Sample 2 Mass Retained (grams)
+ 4.5 mm	40.1 g	23.4 g
+ 4 mm	21.5 g	17.7 g
+ 3.55 mm	36.4 g	23.4 g
+ 3.15 mm	32.2 g	29 g
+ 2 mm	95.7 g	102.4 g
+1.4 mm	41.9 g	58.6 g
+ 0.71 mm	57.2 g	76.8 g
+ 0.5 mm	22.8 g	25.6 g
+ 0.25 mm	54.4 g	38.8 g
+ 0.15 mm	35.4	26.8
+ 0.125 mm	17.9	10.7
- 125 mm on (pan)	42.4	66.8

Table 4.1 particle size distribution after crushing

Grinding Processes

This analyses as Sample1 obtained finer particles of 4.5 mm and 3.55 mm while Sample 2 showed a greater concentration of finer particles, especially in the +0.71 mm and pan (-0.125 mm) fraction. Also For both samples, the greatest amount of mass was recored at the 2mm sieve which for sample one was 95.7g and sample two showed 102.4g which indicates there is a high proportion of mid-range sized particles. It can also be seen from the table that sample 2 generally is finer in particle size and most likely retains small sieves compared to sample 1.

Table 4.2 particle size distribution after grinding

Sieve Size (mm)	Condition-1 Mass Retained (grams)	Condition-2 Mass Retained (grams)	Condition-3 Mass Retained (grams)	Condition-4 Mass Retained (grams)
+ 1.4 mm	1.4 g	0.2 g	9.7 g	49.2 g
+ 1 mm	2.1 g	2.8 g	13.6 g	27.3 g
+ 0.71 mm	3.8 g	4.2 g	15.6 g	22.2 g
+ 0.5 mm	9.3 g	6.9 g	19.3 g	20.1 g
+ 0.25 mm	61.7 g	18.6 g	62.5 g	26.6 g
+ 0.15 mm	65.3 g	68.2 g	46.8 g	29.9 g
- 0.15 mm/pan	106 g	149.1 g	82.5 g	74.7 g

after milling/grinding sieve analysis to determine size distribution

sieve time to all four samples is 10 minute

4.1.1. Particle Size Distribution Analysis

Particle size distribution (PSD) analysis is essential after crushing and grinding processes to assess the efficiency of size reduction and to ensure the sample meets the required specifications for subsequent further processing and testing (XRD and AAS analysis). Below is a detailed procedure on (figure 4.1) shown for conducting PSD analysis after crushing and grinding, which includes methods such as sieving depending on available equipment.

Clean trays to collect sieved material.

Figure 4.1 PSD after grinding and sieve analysis

To calculate the particle size distribution and determine the percentage of material passing through each sieve, we need to calculate:

Mass retained: The variation in the quantity of material retained on each successive sieve.

- **Percentage Retained (%)** $= \frac{\text{Mass Retained on Sieve}}{\text{Total Mass Feed}} \times 100$
- **Cumulative mass:** The sum of the mass retained up to each sieve.
- **Percentage passing:** 100%−Percentage Retained

Particle Size Distribution Analysis after crushing and all calculated resuts shown on (Table 4.3) below.

For (**Sample 1),** the total mass is 500 grams.

Sieve Size (mm)	Mass Ret (gm)	Ret (%)	Cum. Mass(g)	Cum. Ret (%)	Cum. Pass (%)
+4.5 mm	40.1 gm	8.02	40.1 gm	8.02	91.98
+4 mm	21.5 gm	4.30	61.6 gm	12.32	87.68
+3.55 mm	36.4 gm	7.28	98.0 gm	19.60	80.40
+3.15 mm	32.2 gm	6.44	130.2 gm	26.44	73.56
+2 mm	95.7 gm	19.14	225.9 gm	45.58	54.42
+1.4 mm	41.9 gm	8.38	267.8 gm	53.96	46.04
+0.71 mm	57.2 gm	11.44	325.0 gm	65.90	34.10
+0.5 mm	22.8 gm	4.56	347.8 gm	69.46	30.54
+0.25 mm	54.4 gm	10.88	402.2 gm	80.44	19.56
+0.15 mm	35.4 gm	7.08	437.6 gm	87.52	12.48
+0.125 mm	17.9 gm	3.58	455.5 gm	91.10	8.90
-0.125 mm	42.4 gm	8.48	497.9 gm	99.58	0.42

Table 4.3 PSD analysis after crushing for (sample 1)

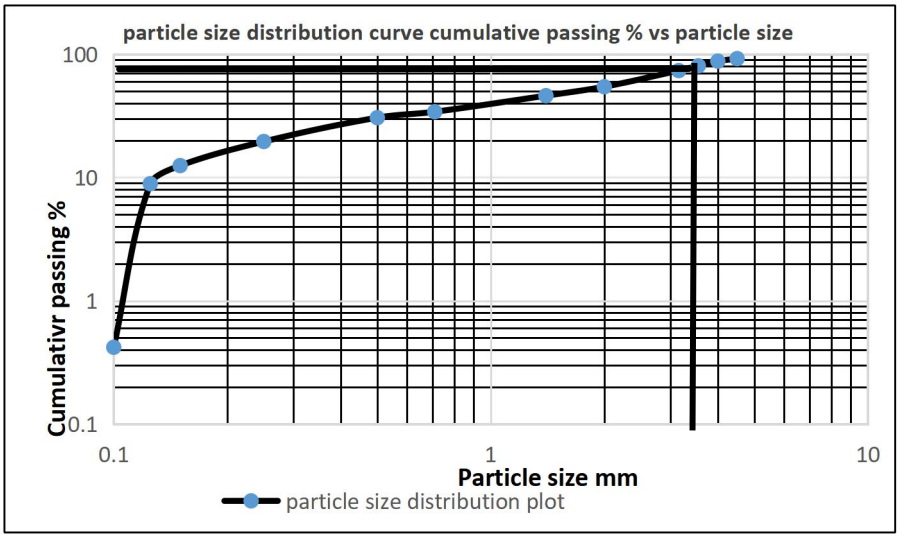

Figure 4.2 PSD analysis after crushing for sample 1 plot

Total sample mass = 500 grams = 0.5 kg

P80 = 3.5 mm = 3500 micron

F80 = 4.5 mm = 4500 micron

Work index (Wi) is 11.4 kWh/t for a pegmatite.

In this section, we are going to calculate the power of the crusher in the circuit, as well as the specific energy consumption and post-crushing Particle Size Distribution (PSD) through systematic steps.

For Bond's Law Calculations, Above mentioned Energies Holes will be used all together for energy consumption calculation.

$W = Wi(\frac{10}{\sqrt{P80}} - \frac{10}{\sqrt{F80}})$

Where:

W = Specific energy required (kWh/ton)

Wi = Work index (kWh/ton)

P80 = Product size (µm)

F80 = Feed size (µm)

$W = Wi(\frac{10}{\sqrt{3500}} - \frac{10}{\sqrt{4500}})$

$W = 11.4\ kWh/t(\frac{10}{\sqrt{3500}} - \frac{10}{\sqrt{4500}})$

$W = \frac{11.4\ KWt/t \times 10}{59.16} - \frac{11.4 kwt/t \times 10}{67}$

$W \approx 0.23$ kWh/ton

So, the specific energy required for crushing is approximately 0.23 **kWh/ton**.

Calculating the Energy Used for the Sample 1

Power = W × tonnage thus tonnage.

If the total sample mass is 500 grams (0.5 kg) and the energy consumption is 0.23 kWh/ton, we can estimate the power required for the sample.

The power required per kg (based on 1 ton = 1000 kg) is:

$P = 0.23\ kWh/ton \times 0.5kg\ \frac{0.5\ kg}{1000kg/ton}$

$P = 0.23 \times 0.0005$ kWh

$P = 0.000113$ kWh ≈ 0.113 Wh

So, the power required to crush the 500 g sample is approximately **0.000113 kWh ≈ 0.113 Wh.**

For Sample 2, the total mass is 500 grams.

Table 4.4 PSD analysis after crushing for (sample 2)

Sieve Size (mm)	**Mass Retained (g)**	**Percentage Retained (%)**	**Cumulative Mass (g)**	**Cumulative Retained (%)**	**Cumulative Passing (%)**
+4.5 mm	23.4	4.68%	23.4	4.68%	95.32%
+4 mm	17.7	3.54%	41.1	8.22%	91.78%

Sieve Size (mm)	Mass Retained (g)	Percentage Retained (%)	Cumulative Mass (g)	Cumulative Retained (%)	Cumulative Passing (%)
+3.55 mm	23.4	4.68%	64.5	12.90%	87.10%
+3.15 mm	29.0	5.80%	93.5	18.70%	81.30%
+2 mm	102.4	20.48%	195.9	39.18%	60.82%
+1.4 mm	58.6	11.72%	254.5	50.90%	49.10%
+0.71 mm	76.8	15.36%	331.3	66.26%	33.74%
+0.5 mm	25.6	5.12%	356.9	71.38%	28.62%
+0.25 mm	38.8	7.76%	395.7	79.14%	20.86%
+0.15 mm	26.8	5.36%	422.5	84.50%	15.50%
+0.125 mm	10.7	2.14%	433.2	86.64%	13.36%
-0.125 mm	66.8	13.36%	500	100%	0%

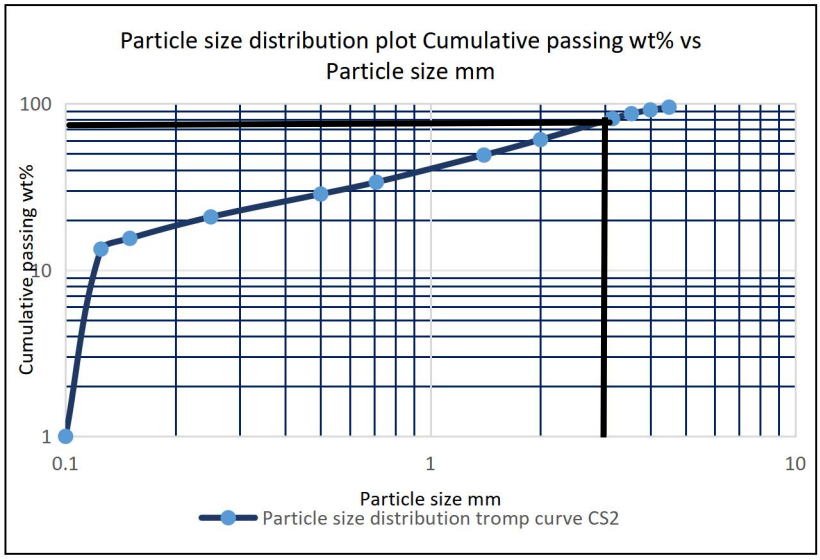

Figure 4.3 PSD Analysis after crushing for sample 2 plot

P80 = 3 mm = 3000 microns F80 = 4.5 mm = 4500 microns

Work index (Wi) for pegmatite = 11.4 kWh/t

In order to determine the required power for each stage of the crusher in the circuit, along with analyzing energy consumption and PSD after crushing, step-wise approach will be adopted.

To estimate energy consumption through Bond's Law,

This can be calculated using Bond's law for energy consumption:

$$W = Wi\left(\frac{10}{\sqrt{P80}} - \frac{10}{\sqrt{F80}}\right)$$

Where:

W = Specific energy required (kWh/ton)

Wi = Work index (kWh/ton)

P80 = Product size (µm)

F80 = Feed size (µm)

$W = Wi(\frac{10}{\sqrt{3000}} - \frac{10}{\sqrt{4500}})$

$W = 11.4\ kWh/t(\frac{10}{\sqrt{3000}} - \frac{10}{\sqrt{4500}})$

$W = \frac{11.4\ KWt/t \times 10}{54.77} - \frac{11.4 kwt/t \times 10}{67}$

$W \approx 0.38$ kWh/ton

So, the specific energy required for crushing is approximately 0.38 **kWh/ton**.

Calculating the Power Used for the Sample 2

Power = W × tonnage thus tonnage.

If the total sample mass is 500 grams (0.5 kg) and the energy consumption is 0.38 kWh/ton, we can estimate the power required for the sample.

The power per kg (based on 1 ton = 1000 kg) is:

$P = 0.38 kWh/ton \times 0.5 kg\ \frac{0.5\ kg}{1000 kg/ton}$

$P = 0.38 \times 0.0005$ kWh

$P = 0.0045$ kWh ≈ 4.5 Wh

So, the power required to crush the 500 g sample is approximately **0.0045 kWh ≈ 4.5 Wh.**

Interpretations for crushing result:

At the crushing stage, two samples (Sample 1 and Sample 2) were studied in terms of the mass of each sieve, as well as the cumulative passing percentage which serves as a measure for determining the distribution of particles size after crushing. The P80 and F80 values are important metrics for determining whether the reduction from the crushing process has been achieved to the intended level.

Sample 1 had a P80 of 3.5 mm while F 80 was 4.5 mm. Sample 2 had a slightly finer P80 of 3 mm and an F80 of 4.5 mm. This means that Sample 2 achieved finer particle size than Sample 1, thus more efficient reduction during the crushing process.

The specific energy needed to be expended for crushing, computed using Bond's law, was considerably low for Sample 1 (0.23 kWh/ton) than Sample 2 (0.38 kWh/ton). This indicates that Sample 2 required more energy to obtain finer particles.

Particle Size Distribution Analysis after grinding/milling:

In regard to each sample, we will take these steps to complete a thorough Particle Size Analysis with the given scope of work involving Percentage Retained (%), Cumulative Mass (g), and

Cumulative % Passing (%). These columns will give a complete picture of the distribution of sizes and the amount of mass that passed through the sieve.

Percentage Retained (%) $= \frac{\textbf{Mass Retained on Sieve}}{\textbf{Total Mass Feed}} \times 100$

Cumulative Mass (g): This is a running total of the mass retained up to that sieve.

❖ **(Sample 1) (350 rpm, 20 minutes):**

Total mass feed to ball mill = 250 g

Table 4.5 PSD analysis after grinding for (sample 1)

Sieve Size (mm)	Mass Retained (g)	Percentage Retained (%)	Cumulative Mass (g)	Cumulative Retained (%)	Cumulative Passing (%)
+1.4 mm	1.4	0.56	1.4	0.56	99.44
+1 mm	2.1	0.84	3.5	1.4	98.6
+0.71 mm	3.8	1.52	7.3	2.92	97.08
+0.5 mm	9.3	3.72	16.6	6.64	93.36
+0.25 mm	61.7	24.68	78.3	31.32	68.68
+0.15 mm	65.3	26.12	143.6	57.44	42.56
-0.15 mm	106	42.4	249.6	99.84	0.16

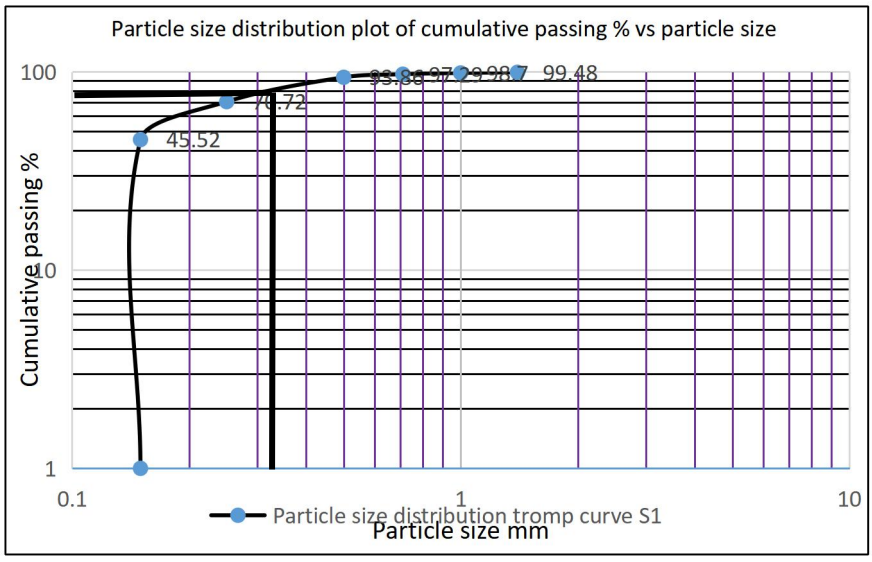

Figure 4.4 PSD Analysis after grindingfor sample 1 plot

P80 = 0.32 mm = 320 microns

F80 = 1.4 mm = 1400 microns

To calculate the mill power required for the circuit and the specific energy consumption, we need to apply the Bond Work Index formula and consider the information you provided about the mill operation and feed material.

The Bond Work Index formula can be used to estimate the energy required to grind the ore in the mill:

$$W = Wi\left(\frac{10}{\sqrt{P80}} - \frac{10}{\sqrt{F80}}\right)$$

$W = Wi(\frac{10}{\sqrt{320}} - \frac{10}{\sqrt{1400}})$

Work index (Wi) for pegmatite = 11.4 kWh/t

$W = 11.4\ kWt/t(\frac{10}{17.9} - \frac{10}{37.4})$

$W = \frac{114}{17.9} - \frac{114}{37.4}$

$W \approx 3.35$ kWh/ton

So, the energy required for crushing is approximately 3.35 **kWh/ton**.

Calculating the Power Used for the Sample 1

Power = W × tonnage thus tonnage.

If the total sample mass is 250 grams (0.25 kg) and the energy consumption is 3.35 kWh/ton, we can estimate the power required for the sample.

The power required per kg (based on 1 ton = 1000 kg) is:

$P = 3.35 kWh/ton \times \frac{0.25\ kg}{1000 kg/ton}$

$P = 3.35 \times 0.0025$ kWh

$P = 0.0084$ kWh ≈ 8.4 Wh

So, the Power required to grind the 250 g sample 1 is approximately 0.0084 kWh ≈ 8.4 Wh.

Condition 2 (Sample 2) (700 rpm, 20 minutes):

Total mass feed to ball mill = 250 g

Table 4.6 PSD analysis after grinding for (sample 2)

Sieve Size (mm)	**Mass Retained (g)**	**Percentage Retained (%)**	**Cumulative Mass (g)**	**Cumulative Retained (%)**	**Cumulative Passing (%)**
+1.4 mm	0.2	0.08%	0.2	0.08%	99.92%
+1 mm	2.8	1.12%	3.0	1.20%	98.80%
+0.71 mm	4.2	1.68%	7.2	2.88%	97.12%
+0.5 mm	6.9	2.76%	14.1	5.64%	94.36%
+0.25 mm	18.6	7.44%	32.7	13.08%	86.92%
+0.15 mm	68.2	27.28%	100.9	40.36%	59.64%
-0.15 mm	149.1	59.64%	250.0	100%	0%

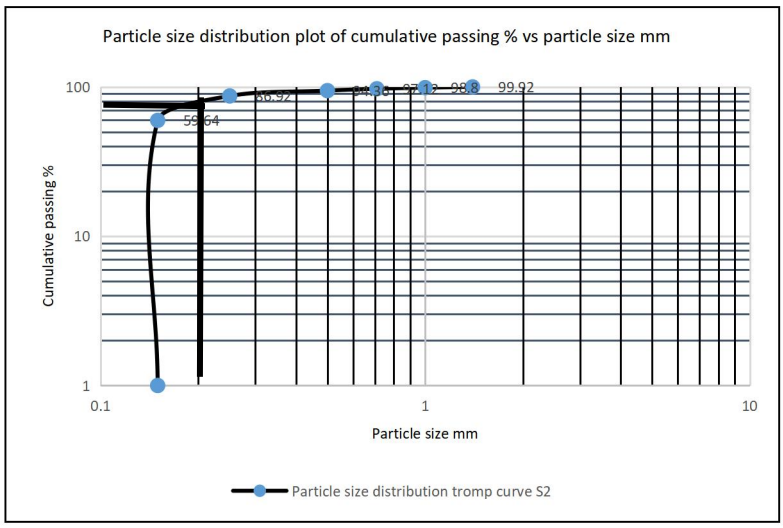

Figure 4.5 PSD Analysis after grinding sample 2 plot

P80 = 0.2 mm = 200 microns

F80 = 1.4 mm = 1400 microns

To calculate the mill power required for the circuit and the specific energy consumption, we need to apply the Bond Work Index formula and consider the information you provided about the mill operation and feed material.

$W = Wi(\frac{10}{\sqrt{P80}} - \frac{10}{\sqrt{F80}})$

$W = Wi(\frac{10}{\sqrt{200}} - \frac{10}{\sqrt{1400}})$

Work index (Wi) for pegmatite = 11.4 kWh/t

$W = 11.4\ kWt/t(\frac{10}{14.14} - \frac{10}{37.4})$

$W = \frac{114}{14.14} - \frac{114}{37.4}$

$W \approx 5.01$ kWh/ton

So, the specific energy required for crushing is approximately 5.01 **kWh/ton**.

Calculating the Power Used for the Sample 2

Power = W × tonnage thus tonnage.

If the total sample mass is 250 grams (0.25 kg) and the energy consumption is 5.01 kWh/ton, we can estimate the power required for the sample.

The power required per kg (based on 1 ton = 1000 kg) is:

$P = 5.01 kWh/ton \times \frac{0.25\ kg}{1000 kg/ton}$

$P = 5.01 \times 0.0025$ kWh

$P = 0.0125$ kWh ≈ 12.5 Wh

So, the power required to grind the 250 g sample 2 is approximately 0.0125 kWh ≈ 12.5 Wh.

Condition 3 (Sample 3)

1050 rpm, 20 minutes:

Total mass feed to ball mill = 250 g

Table 4.7 PSD analysis after grinding for (sample 3)

Sieve Size (mm)	Mass Retained (g)	Percentage Retained (%)	Cumulative Mass (g)	Cumulative Retained (%)	Cumulative Passing (%)
+1.4 mm	9.7 g	3.88%	9.7 g	3.88%	96.12%
+1 mm	13.6 g	5.44%	23.3 g	9.32%	90.68%
+0.71 mm	15.6 g	6.24%	38.9 g	15.56%	84.44%
+0.5 mm	19.3 g	7.72%	58.2 g	23.28%	76.72%
+0.25 mm	62.5 g	25.00%	120.7 g	48.28%	51.72%
+0.15 mm	46.8 g	18.72%	167.5 g	67.00%	33.00%
-0.15 mm	82.5 g	33.00%	250.0 g	100.00%	0.00%

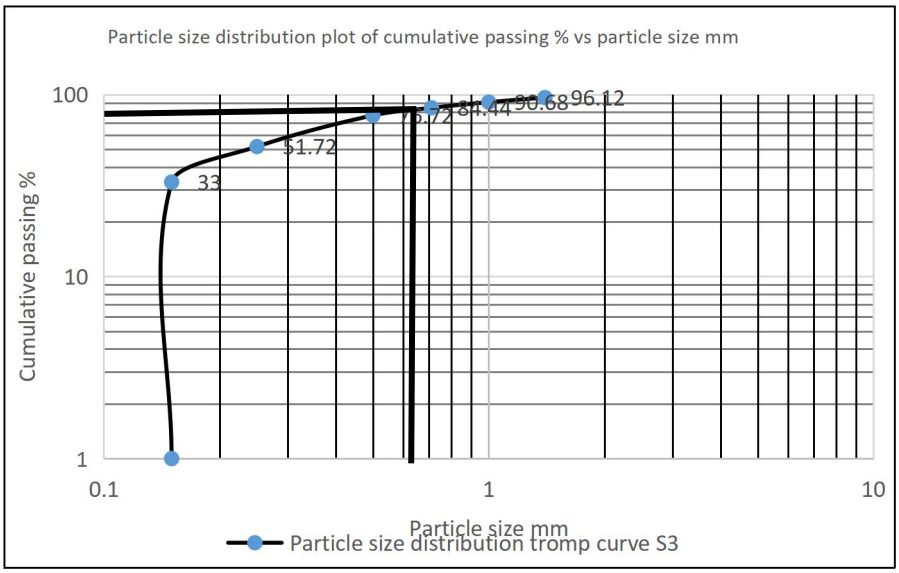

Figure 4.6 PSD Analysis after grinding sample 3 plot

P80 = 0.62 mm = 620 microns

F80 = 1.4 mm = 1400 microns

To calculate the mill power required for the circuit and the specific energy consumption, we need to apply the Bond Work Index formula and consider the information you provided about the mill operation and feed material.

$W = Wi(\frac{10}{\sqrt{P80}} - \frac{10}{\sqrt{F80}})$

$W = Wi(\frac{10}{\sqrt{620}} - \frac{10}{\sqrt{1400}})$

Work index (Wi) for pegmatite = 11.4 kWh/t

$W = 11.4\ kWt/t(\frac{10}{24.9} - \frac{10}{37.4})$

$W = \frac{114}{24.9} - \frac{114}{37.4}$

$W \approx 1.53$ kWh/ton

So, the energy required for crushing is approximately 1.53 **kWh/ton**.

Calculating the Power Used for the Sample 3

The power required for the circuit can be calculated as follows:

Power = W × tonnage thus tonnage.

If the total sample mass is 250 grams (0.25 kg) and the energy consumption is 1.53 kWh/ton, we can estimate the total power for the sample.

The power required per kg (based on 1 ton = 1000 kg) is:

$P = 1.53 \text{ kWh/ton} \times \frac{0.25 \text{ kg}}{1000 \text{kg/ton}}$

$P = 1.53 \times 0.0025$ kWh

$P = 0.0038$ kWh ≈ 3.8 Wh

So, the power required to grind the 250 g sample 3 is approximately **0.0038 kWh ≈ 3.8 Wh.**

Sample 4 (350 rpm, 20 minutes, coarser feed size 2–4.5 mm):

Total mass feed to ball mill = 250 g

Table 4.8 PSD after grinding for (sample 4)

Sieve Size (mm)	**Mass Retained (g)**	**Percentage Retained (%)**	**Cumulative Mass (g)**	**Cumulative Retained (%)**	**Cumulative Passing (%)**
+1.4 mm	49.2 g	19.68%	49.2 g	19.68%	80.32%
+1 mm	27.3 g	10.92%	76.5 g	30.60%	69.40%
+0.71 mm	22.2 g	8.88%	98.7 g	39.48%	60.52%
+0.5 mm	20.1 g	8.04%	118.8 g	47.52%	52.48%
+0.25 mm	26.6 g	10.64%	145.4 g	58.16%	41.84%
+0.15 mm	29.9 g	11.96%	175.3 g	70.12%	29.88%
-0.15 mm	74.7 g	29.88%	250.0 g	100.00%	0.00%

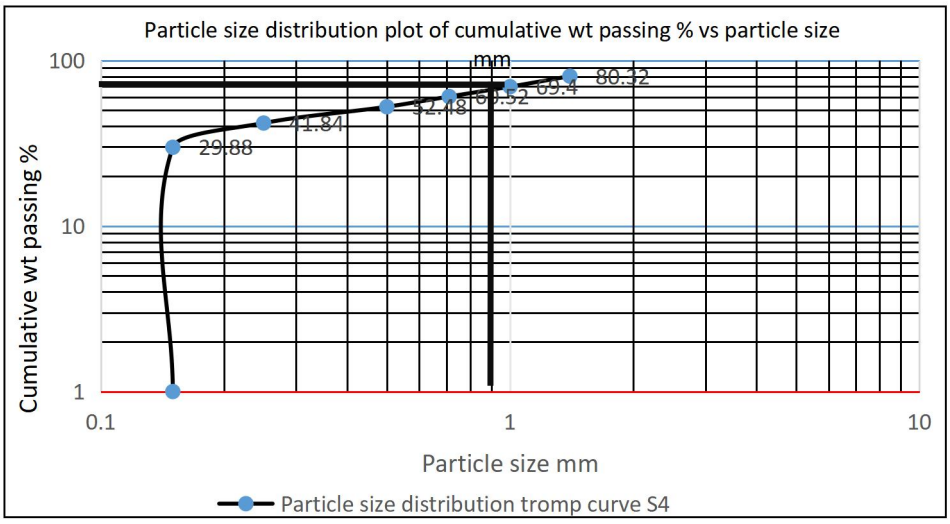

Figure 4.7 PSD Analysis after grinding for sample 4 plot

P80 = 1.3 mm = 1300 microns

F80 = 4.5 mm = 4500 microns

To calculate the mill power required for the circuit and the specific energy consumption, we need to apply the Bond Work Index formula and consider the information you provided about the mill operation and feed material.

$W = Wi(\frac{10}{\sqrt{P80}} - \frac{10}{\sqrt{F80}})$

$W = Wi(\frac{10}{\sqrt{1300}} - \frac{10}{\sqrt{4500}})$

Work index (Wi) for pegmatite = 11.4 kWh/t

$W = 11.4\ kWt/t(\frac{10}{24.9} - \frac{10}{37.4})$

$W = \frac{114}{36.1} - \frac{114}{67.1}$

$W \approx 1.46$ kWh/ton

So, the energy required for crushing is approximately 1.46 **kWh/ton**.

Calculating the Power Used for the Sample 4

The power required for the circuit can be calculated as follows:

Power = W × tonnage thus tonnage.

If the total sample mass is 250 grams (0.25 kg) and the energy consumption is 1.46 kWh/ton, we can estimate the power required for the sample.

The power required per kg (based on 1 ton = 1000 kg) is:

$P = 1.46\ kWh/ton \times \frac{0.25\ kg}{1000 kg/ton}$

$P = 1.46 \times 0.0025$ kWh

$P = 0.003365$ kWh ≈ 3.365 Wh

So, the total power required to grind the 250 g sample 3 is approximately 0.003365 kWh ≈ **3.365 Wh.**

Interpretations for crushing result:

At the crushing stage, two samples (Sample 1 and Sample 2) were studied in terms of the mass of each sieve, as well as the cumulative passing percentage which serves as a measure for determining the distribution of particles size after crushing. The P80 and F80 values are important metrics for determining whether the reduction from the crushing process has been achieved to the intended level.

Sample 1 had a P80 of 3.5 mm while F 80 was 4.5 mm. Sample 2 had a slightly finer P80 of 3 mm and an F80 of 4.5 mm. This means that Sample 2 achieved finer particle size than Sample 1, thus more efficient reduction during the crushing process.

The specific energy needed to be expended for crushing, computed using Bond's law, was considerably low for Sample 1 (0.23 kWh/ton) than Sample 2 (0.38 kWh/ton). This indicates that Sample 2 required more energy to obtain finer particles.

In regard to each sample, we will take these steps to complete a thorough Particle Size Analysis with the given scope of work involving Percentage Retained (%), Cumulative Mass (g), and Cumulative % Passing (%). These columns will give a complete picture of the distribution of sizes and the amount of mass that passed through the sieve.

Impact of Feed Size on Grinding Efficiency:

In Sample 4 which was remilled with coarser feed size (2–4.5 mm) exhibited the highest P80 value of 1.3 mm. Generally, grinding coarser feed is associated with increased energy expenditure and results in coarser final products. Sample 4 total energy spend of approximately 0.003365 kWh is lower than finer energy samples, but higher than the energy for Sample 1, demonstrating a coarser grind.

From the analysis, we can observe a number of important trends already:

Energy Consumption and Granulation:

As with most granulation processes, energy consumption is highest for the finer grind (Sample 2 with P80 of 200 microns). Here we see a distinct mark related to spent energy. This indicates that the desired finer particle size increases the required energy, illuminating the interrelationship between energy efficiency and process optimization required in grinding processes.

Effect of Spindle Speed:

Lower P80 values (200 microns in Sample 2 and 620 microns in Sample 3) stem from higher spindle speeds, indicating a gradual enhancement of productivity/energy ratio. These results suggest higher values of spindle speed may improve grinding efficiency but at the cost of increased energy consumption.

After Crushing and Grinding Particle Size Distribution:

The PSD for the crushing step (Samples 1 and 2) exhibited an relatively broad distribution and retained a significant portion of material on the coarser sieves (8-20%). The distribution was made significantly finer after grinding, with marked decreases in the amount of material passing through finer sieves (0.125 mm and smaller). The results indicates that the milling process is effective in reducing the particle sizes to the required specifications.

Effects of Feed Size:

Sample 4's coarse feed content lead to a larger P80 value which means that larger coarser feed sizes do not undergo sufficient fine grinding and instead spend more energy to reduce the particle size.

4.2. Analytical Techniques

4.2.1. Mineralogical Analysis

X-ray Diffraction (XRD) Analysis Description

The X-ray diffraction (XRD) analysis conducted the representative samples and quantify the mineralogical composition of lithium-bearing pegmatite from the Burkuke, Sidama Regional state, Ethiopia. The diffractogram (Figure X) displays multiple sharp and intense peaks, indicating a crystalline and multi-phase composition.

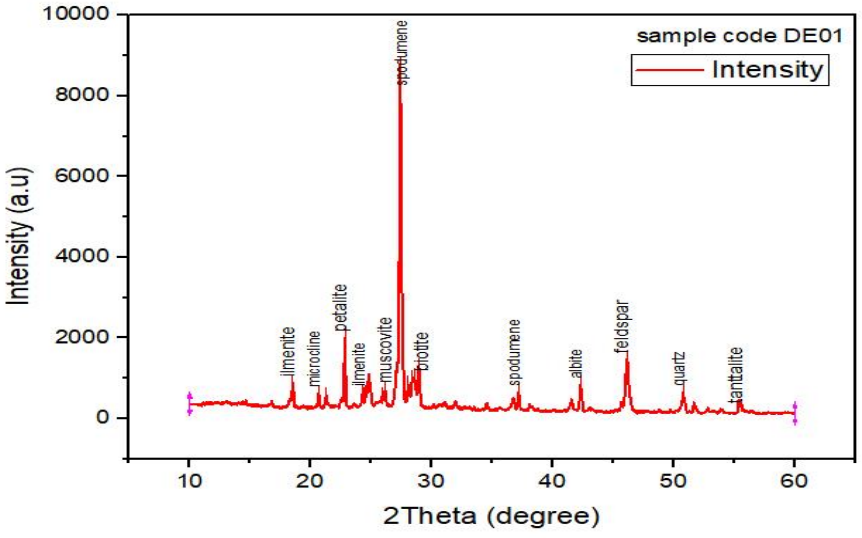

Figure 4.8 XRD Identified phases and their amounts (%) sample code DE01

Interpretation for XRD results of mineralogical analysis in (figure 4.9) shows that the X-ray diffraction (XRD) pattern of sample DE02 reveals a mineral assemblage dominated by

spodumene, shown by multiple strong peaks, particularly near the 2θ = 28–30° region. **Feldspar**, **muscovite**, and **beryl** also exhibit strong peaks in this range, indicating their significant presence.

Table 4.9 XRD mineralogical (phase) and Elemental wt% identification sample DE01

Phase	Formula	Amount (%)		Element	Amount (Weight %)
Spodumene	$LiAl(SiO_3)_2$	30.1		O	29.8%
Microcline	$KAlSi_3O_8$	10.9		Si	17.3%
Albite	$NaAlSi_3O_8$	6.9		Al	7.8%
Feldspar	$(Sr,Na)(Al1.74Si2.26)O_8$	6.7		K	1.9%
Ilmenite	$FeTiO_3$	2.6		Sr	1.6%
Muscovite	$KAl_2(AlSi_3O_{10})(OH)_2$	2.6		Li	0.23%
Petalite	$AlLiO_{10}Si_4$	1.3		Fe	1.1%
Biotite	$K(AlMgFeMn)(Si_2Ti)O_{10}(OH,F)_2$	0.7		Ti	0.8%
Tantalite-(Mn)	$Fe_{0.09}Mn_{0.88}Nb_{0.28}O_6Ta_{1.72}$	0.2		Na	0.6%
Quartz	SiO_2	0.1		Ta	0.1%
Unidentified	-	11.7		Mg	0.1%

The XRD results show in (Table 4.9) the sample DE01 contains several mineral phases with varying composition and relative abundances. The sample contains a rich amount of spodumene 30.1 per cent which indicates high lithium content along with petalite and some muscovite. Feldspars microcline and albite offer silicon and aluminum and in turn, Ilmenite, biotite, and tantalite supply iron, titanium and tantalum. An 11.7% fraction of unidentified material is indicative of some undisclosed or ill-defined complex mineral phases. With regard to lithium bearing minerals, sample DE01 has a dominant concentration of spodumene. There is also microcline and petalite which are feldspar related minerals, along with quartz and biotite in smaller amounts. The sample also contains large area of unidentified peak (11.7%) which needs further attention.

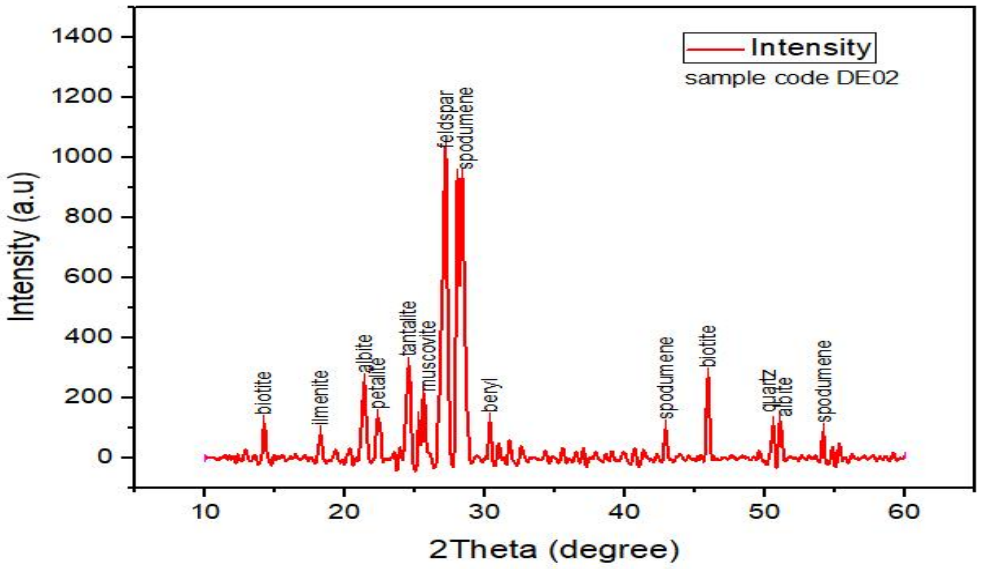

Figure 4.9 XRD Identified phases and their amounts (%) sample code DE02

The interpretation of XRD results of mineralogical analysis in (figure 4.10) above shows that sample code DE02 X-ray diffraction (XRD) showed prominent and sharp peaks which suggest well defined crystallized minerals. The major peaks of 2θ = 27–30° were confirmed to be posidomene and feldspar, hence these were confirmed as the principal constituents. Other notable phases include muscovite, berly, petalite, tantalite, ilmenite, biotite and clquartz that account for the remainder of the 2θ range. The presence of lithium bearing minerals (spodumene, petalite, muscovite) and secondary phases (ilmenite, biotite, tantalite) indicate a complex, lithium-rich pegmatitic rock. This pattern corroborates earlier compositional data which indicated a dominance of spodumene and various accessory minerals.

Table 4.10 XRD Mineralogical (phase) and Elemental wt% identification sample DE02

Phase	Formula	Amount (%)		Element	Amount (Weight %)
Muscovite	$Al_3K_{0.5}O_{12}Si_3$	24.8		O	46.9%
Feldspar	$(Sr,Na)(Al_{1.74}Si_{2.26})O_8$	22.5		Si	28.1%
Albite	$NaAlSi_3O_8$	11.8		Al	12.3%
Beryl	$Al_2Be_3O_{24}Si_{12}$	11.6		Sr	5.3%
Quartz	SiO_2	11.3		K	3.0%
Spodumene	$LiAl(SiO_3)_2$	10.3		Fe	1.1%
Biotite	$K(AlMgFeMn)(Si_2Ti)O_{10}(OH,F)_2$	6.1		Na	1.1%
Tantalite-(Mn)	$Fe_{0.09}Mn_{0.88}Nb_{0.28}O_6Ta_{1.7}$	0.7		Mg	0.7%
Ilmenite	$FeTiO_3$	0.7		Ta	0.5%
Unidentified	-	16.7		Be	0.4%
				Li	0.13%
				Ti	0.1%
				Mn	0.1%

Interpretation for XRD results of mineralogical analysis in (Table 4.10) above shows that the sample composition is dominated by **muscovite (24.8%)** and **feldspar (22.5%)**, contributing to the high oxygen (46.9%) and silicon (28.1%) content. **Albite (11.8%)**, **beryl (11.6%)**, and **quartz (11.3%)** further increase the aluminum and silicon levels, with beryl adding notable **beryllium (0.4%)** and **strontium (5.3%)**. **Spodumene (10.3%)**, a key lithium source, aligns with the observed **Li (0.13%)**, while **biotite (6.1%)** and trace **ilmenite (0.7%)** introduce **iron (1.1%)**, **magnesium (0.7%)**, and **titanium (0.1%)**. Minor **tantalite-(Mn) (0.7%)** provides **tantalum (0.5%)** and **manganese (0.1%)**. The **16.7% unidentified fraction** suggests additional complex or amorphous phases not resolved in the current analysis.

Sample DE02 shows a similar mineral distribution but with a slightly higher proportion of muscovite and feldspar.

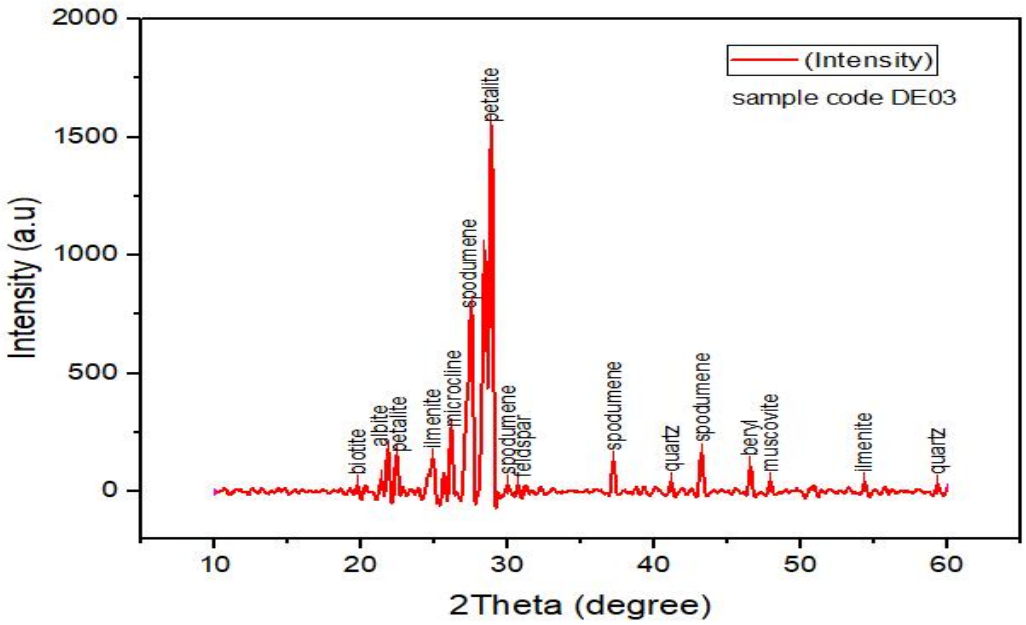

Figure 4.10 XRD Identified phases and their amounts(%) sample DE03

Interpretation for XRD results of mineralogical analysis in (figure 4.11) above shows that the XRD pattern for **sample DE03** reveals a mineral assemblage dominated by **petalite**, which shows the highest intensity peak around **2θ = 28–30°**, indicating it is the most abundant and well-crystallized phase. **Spodumene** is also present with multiple sharp peaks, confirming this sample is rich in lithium-bearing minerals. Additional phases include **microcline**, **albite**, and **quartz**, suggesting a significant presence of feldspar and silicate minerals. **Ilmenite**, **biotite**, **muscovite**, and **beryl** are observed as minor constituents, indicating accessory iron, titanium, and mica minerals. The distribution and sharpness of peaks suggest a well-crystallized, pegmatitic origin with strong lithium mineralization.

Table 4.11 XRD Mineralogical(phase) and Elemental wt% identification Sample DE03

Phase	Formula	Amount (%)		Element	Amount (Weight %)
Muscovite	$Al_3K_{0.5}O_{12}Si_3$	22.7		O	46.8%
Albite	$NaAlSi_3O_8$	22.7		Si	25.4%
Feldspar	$(Sr,Na)(Al_{1.7}Si_{2.3})O_8$	14.0		Al	12.2%
Spodumene	$LiAl(SiO_3)_2$	12.6		Sr	3.3%
Biotite	$K(AlMgFeMn)(Si_2Ti)O_{10}(OH,F)_2$	10.0		K	3.1%
Beryl	$Al_2Be_3O_{18}Si_6$	6.6		Fe	2.9%
Quartz	SiO_2	5.7		Na	2.0%
Ilmenite	$FeTiO_3$	4.5		Ti	1.4%
Tantalite	$Fe_{0.1}Mn_{0.9}Nb_{0.3}O_6Ta_{1.7}$	1.2		Mg	1.1%
Unidentified	-	4.0		Ta	0.8%
				Li	0.2%
				Be	0.3%
				Mn	0.1%
				Nb	0.1%

The interpretation of XRD results from the mineralogical analysis in (Table 4.11) above indicates that the composition of sample DE03 is characterized by muscovite and albite, each at 22.7%, which explains the high oxygen, 46.8%, and silicon, 25.4%, content. Biotite, 10% and spodumene, 12.6%, compose the aluminum and potassium content, but also serve as a key source of lithium with a total Li composition of 0.2%. Accessory minerals like beryl contribute to the total sample composition as well Na and Fe through 2.0% and 2.9%, respectively, while increasing ilmenite brings the total to 1.4%. Rare minerals consisting of tantalites contribute 1.2% to the total Ta composition of 0.8% whilst Mn and Nb lurk in the sample suggesting rare scattered metals. The remaining 4% seems to lie in unexplored scope which indicates vaguely crystalline material. The sample as a whole seems to showcase a lithium peek granulite with different accessory phases. Interestingly, extracts like spodumene and feldspar, known for their lithium bearing potential, bring it up and enable describing it as a lithium-bearing pegmatite with diverse ilmenite.

Sample DE03 contains a variety of phases, bowl-shaped muscovite alongside alsdite while exposing almondine and sanidine as the more recessed phases. On the over side, the beryl as well as quartz ilimite spindle bolstered marks open its silicate-rich composition. The 4% unidentified peak is a strong indicator that nearly minor phases exist ranging from proprietary mark bearings but didn't connect to possible listed marks. Rather speculatively, alongside sodium and iron could compel to use to explain mantle metals.

4.2.2. Chemical Analysis

1. Complete silicate analysis

Analytical methods employed included $LiBO_2$ fusion, HF attack, gravimetric analysis, calorimetric analysis, and atomic absorption spectroscopy (AAS) shown on (Table 4.12) below.

Table 4.12 Geochemical result of AAS analysis of Burkuke pegmatite

Collector's Code	SiO_2 (%)	Al_2O_3 (%)	Fe_2O_3 (%)	CaO (%)	MgO (%)	Na_2O (%)	K_2O (%)	MnO (%)	P_2O_3 (%)	TiO_2 (%)	Li_2O (%)	H_2O (%)	LOI (%)	Sample Weight
D-Z-01	76.26	15.10	0.88	0.50	<0.01	2.74	3.66	0.02	<0.01	0.20	0.09	0.13	1.58	100 gm

The given elements were classified as major and minor oxides with the AAS technique providing exceptional accuracy and precision. Geochemical analysis indicated that the sample had high concentrations of silicon (SiO2), aluminum (Al2O3), and potassium (K2O) as well as moderate amounts of sodium (Na2O). The sample is estimated to contain 0.09% lithium oxide (Li2O), which is relevant for estimating the possibility of lithium recovery from this pegmatite. The sample also contains trace amounts of other elements such as iron (Fe2O3), calcium (CaO), and titanium (TiO2).

To infer the geochemical composition,

The results from the geochemical AAS analysis conducted on a Burkuke pegmatite sample uncover these findings:

Quartz being the allied constituent in pegmatitic deposits, alongside the major ore quantitative exceeding 76% of the composition contains Silicon Dioxide (SiO2). Furthermore, Aluminum Oxide (Al2O3) with a value of 15.10% indicates the occurrence of feldspar alongside several other alumino silicate minerals in the pegmatite portrayed on (appendix 1).

Focusing on potential lithium extraction as a result of increased demand lithium resources, it can be argued that the presence 0.09% of Lithium Oxide (Li2O) is low but still considerable in relevance. However, the presences of Potassium Oxide (K2O) and Sodium Oxide (Na2O) attest as dominating feldspar, a lithium source bearing mineral.

Moreover, Iron Oxide (Fe2O3) is the other oxides that has emerged from Fe.

Explaining the Differences

Lithium-bearing minerals are characterized with their crystallographic features using X-ray Diffraction (XRD) technology, which also quantifies lithium-ion presence as minerals crystallize or form specific structures. The AAS results quantify lithium at a lower value than XRD methods (0.31%); this discrepancy can be explained within the context of XRD detecting crystallized, accessible, and detachable phases of lithium-bearing minerals.

Lepidolite, spodumene, and other lithium-containing minerals can hold lithium as part of their skeletal structures, where XRD would quantify them mineralically. As XRD physically evaluates crystalline phases, it stands to reason that its readings are inflated vis-a-vis the presence of orderly and crystalline minerals containing lithium.

AAS results measure lithium concentration through absorption at pre-defined wavelengths (0.09% Li). Lower results should not be taken into consideration as an absolute structural breakdown within sensitivity limits of the method are assumed to exist in the dissolution phase prior to the analysis.

Detection of ions usually implies existing free and undeclared boundaries or portions enclosed in lesser soluble geometric forms. This explains the assumption that under those circumstances, AAS should not be able to detect bound forms of lithium hosted within host minerals.

Sensitivity and Detection Limits: XRD, might overestimate the lithium content if it identifies phases rich in lithium but may not detect all forms of lithium, especially if it is present in amorphous or fine-grained material.

Sample Preparation and Chemical State: The sample preparation methods for AAS might not fully dissolve all lithium-bearing minerals, especially if the lithium is locked in more complex mineral structures or phases that do not dissolve easily under the conditions of the analysis.

5. Conclusions and Recommendations

5.1. Conclusions

The study on the Mineralogical Characterization and Comminution Energy requirement of Lithium-Bearing Pegmatite located in the Burkuke locality in Sidama Regional state, Ethiopia show lithium occurence mineral resources. The results underscore the concentration of lithium-containing minerals like spodumene along with a number of other associated elements which increase the economic potential of this deposit. This was revealed by the XRD mineralogical analysis. The other accompanying phases are albite, muscovite, petalite, and feldspar. The quantitative analysis showed the value of some oxides like SiO_2 76.26%, Al_2O_3 15.10%, and Li_2O 0.09% are present. Such findings suggest that in order to foster the enhanced lithum liberation from pegmatite, optimal comminution strategies are particularly important. There is a need to balance between energy usage and particle size reduction for efficient processing without drawing too much energy. To summarize, the Burkuke pegmatite holds considerable lithium resource development potential. Efficient processing strategies, especially in terms of mineral servicing and comminution, are critical to maximizing lithium recovery. The findings of the study highlighted the prospects for sustainable lithium exploitation in this region, furthering Ethiopia's developmental aspirations while also integrating into Internacional demands for battery-grade lithium.

The results from comminution tests which include jaw crushing and ball milling indicate that the efficiency of size reduction per unit of energy consumed is highly dependent on the feed size and milling speed. In jaw crushing, faster speeds (700rpm) produced finer products like (P80 = 200μm) but consumed more energy (5.01kWh/t). On the other hand, lower speeds combined with coarser feed sizes consumed less energy but reduced size more inefficiently.

5.2. Recommendations

1. It is recommended to assess modern grinding alternatives such as high-pressure grinding rolls (HPGR) and vertical roller mills (VRM), which may improve processing efficiency and significantly reduce energy consumption compared to ball mills.
2. The experiment was conducted using a batch ball mill circuit. It is recommended to conduct future experiments in a continuous grinding circuit to more accurately evaluate grinding efficiency and simulate industrial-scale operations.
3. **Process Control:** Implementing more advanced control systems to adjust milling conditions in real-time can further improve efficiency and ensure that both particle size and energy consumption are optimized for the desired outcomes.
4. **Lithium Extraction Potential:** Since spodumene is present in all samples, it is recommended to further investigate the lithium content and assess the potential for economic extraction.
5. Perform comprehensive purity and quality assessments of feldspar and albite to evaluate their feasibility for glass and ceramics manufacturing. Additionally, investigate muscovite and biotite for potential use in electronic applications, focusing on mica-based product development.

6. References

1. Asmare, M., Zegeye, M., & Ketema, A. (2024). Advancement of electrically rechargeable metal-air batteries for future mobility. Energy Reports, 11, 1199–1211. https://doi.org/10.1016/j .egy r.2023.12.067
2. Aylmore, M. G., Merigot, K., Rickard, W. D. A., Evans, N. J., McDonald, B. J., Catovic, E., & Spitalny, P. (2018). Assessment of a spodumene ore by advanced analytical and mass spectrometry techniques to determine its amenability to processing for the extraction of lithium. Minerals Engineering, 119, 137–148. https://doi.org/10.1016/j.mineng.2018.01.010
3. Balaram, V., Santosh, M., Satyanarayanan, M., Srinivas, N., & Gupta, H. (2024). Lithium: A review of applications, occurrence, exploration, extraction, recycling, analysis, and environmental impact. Geoscience Frontiers, 15(5), 101868. https://doi.org/10.1016/j.gsf.2024.101868
4. Bouzahzah, H., Benzaazoua, M., Bussiere, B., & Plante, B. (2014). Prediction of Acid Mine Drainage: Importance of Mineralogy and the Test Protocols for Static and Kinetic Tests. Mine Water and the Environment, 33(1), 54–65. https://doi.org/10.1007/s10230-013-0249-1
5. Breasley, C. M., Martins, T., Linnen, R. L., Deveau, C., Groat, L. A., Koopmans, L., Landry, E., & Moser, D. (2025). The geochemistry, origins and metallurgical implications of different textural types of spodumene-quartz intergrowths (SQUI) from the Tanco pegmatite, Manitoba, Canada. *Ore Geology Reviews*, *180*, 106577. https://doi.org/10.1016/j.oregeorev.2025.106577
6. Dharmapriya, P. L., Disanayaka, D. W. M., Pitawala, H. M. T. G. A., Malaviarachchi, S. P. K., & Subasinghe, N. D. (2025). Genesis, classification, tectonic setting and economic potential of global granitic pegmatites: A review. Evolving Earth, 3, 100059. https://doi.org/10.1016/j.eve.2025.100059
7. Ghorbani, Y., Zhang, S. E., Bourdeau, J. E., Chipangamate, N. S., Rose, D. H., Valodia, I., & Nwaila, G. T. (2024). The strategic role of lithium in the green energy transition: Towards an OPEC-style framework for green energy-mineral exporting countries (GEMEC). Resources Policy, 90, 104737. https://doi.org/10.1016/j.resourpol.2024.104737
8. Gil-Alana, L. A., & Monge, M. (2019). Lithium: Production and estimated consumption. Evidence of persistence. Resources Policy, 60, 198–202. https://doi.org/10.1016/j.resourpol.2019.01.006
9. Goodenough, K. M., Shaw, R. A., Borst, A. M., Nex, P. A. M., Kinnaird, J. A., Van Lichtervelde, M., Essaifi, A., Koopmans, L., & Deady, E. A. (2025). Lithium Pegmatites in Africa: A Review. Economic Geology. https://doi.org/10.5382/econgeo.5133

10. Hajam, Y. A., Kumar, R., & Kumar, A. (2023). Environmental waste management strategies and vermi transformation for sustainable development. Environmental Challenges, 13, 100747. https://doi.org/10.1016/j.envc.2023.100747
11. Jiao, F., Zhang, Z., Wei, Q., & Qin, W. (2024). Key technologies and development trends for efficient flotation recovery of lepidolite. Green and Smart Mining Engineering, 1(3), 273–288. https://doi.org/10.1016/j.gsme.2024.08.002
12. Kapadia, S. (2018). Comminution in mineral processing. Unpublished. https://doi.org/10.13140 /RG.2.2.34991.89760
13. Küster, D., Romer, R. L., Tolessa, D., Zerihun, D., Bheemalingeswara, K., Melcher, F., & Oberthür, T. (2009). The Kenticha rare-element pegmatite, Ethiopia: Internal differentiation, U–Pb age and Ta mineralization. Mineralium Deposita, 44(7), 723–750. https://doi.org/10.1007/s00126-009-0240-8
14. Kwade, A., Möller, M., Müller, J., Hesselbach, J., Zellmer, S., Doose, S., Mayer, J., Michalowski, P., Powell, M., & Breitung-Faes, S. (2023). Comminution and Classification as Important Process Steps for the Circular Production of Lithium Batteries. KONA Powder and Particle Journal, 40(0), 50–73. https://doi.org/10.14356/kona.2023006
15. Koech, A. K., Mwandila, G., Mulolani, F., & Mwaanga, P. (2024). Lithium-ion battery fundamentals and exploration of cathode materials: A review. South African Journal of Chemical Engineering, 50, 321–339. https://doi.org/10.1016/j.sajce.2024.09.008
16. Machado-Vieira, R., Manji, H. K., & Zarate Jr, C. A. (2009). The role of lithium in the treatment of bipolar disorder: Convergent evidence for neurotrophic effects as a unifying hypothesis. *Bipolar Disorders*, *11*(s2), 92–109. https://doi.org/10.1111/j.1399-5618.2009.00714.x
17. Maneta, V., Baker, D. R., & Minarik, W. (2015). Evidence for lithium-aluminosilicate supersaturation of pegmatite-forming melts. Contributions to Mineralogy and Petrology, 170(1), 4. https://doi.org/10.1007/s00410-015-1158-z
18. Marsh, R. A., Vukson, S., Surampudi, S., Ratnakumar, B. V., Smart, M. C., Manzo, M., & Dalton, P. J. (2001). Li ion batteries for aerospace applications. *Journal of Power Sources*, *97–98*, 25–27. https://doi.org/10.1016/S0378-7753(01)00584-5
19. Ministry of Mines (2023). Annual Report on Ethiopia's Mineral Sector Development. Addis Ababa, Ethiopia.
20. Mohammedyasin, M. S. (2017). Geology, Geochemistry and Geochronology of the Kenticha Rare Metal Granite Pegmatite, Adola Belt, Southern Ethiopia: A Review. International Journal of Geosciences, 08(01), 46–64. https://doi.org/10.4236/ijg.2017.81004

21. Montana Bureau of Mines and Geology, & Van Rythoven, A. (2023). Critical mineral: Tantalum. Montana Bureau of Mines and Geology. https://doi.org/10.59691/CCXJ2700
22. Nandihalli, N., Chouhan, R. K., Kuchi, R., & Hlova, I. Z. (2024). Aspects of Spodumene Lithium Extraction Techniques. Sustainability, 16(19), 8513. https://doi.org/10.3390/su16198513
23. Petrakis, E., Alexopoulos, I., Pantelaki, O., Karmali, V., & Komnitsas, K. (2025). Advances in Mineral Processing of Hard-Rock Lithium Ores: A Comprehensive Review. Mining, Metallurgy & Exploration. https://doi.org/10.1007/s42461-025-01227-y
24. Rajhi, S., Legault, M., Mvondo, H., & Potvin, R. (2024). Characterization of pegmatites in the La Motte Batholith area, Preissac-La Corne Plutonic Suite, Abitibi Subprovince and its implications for exploration. Journal of Geochemical Exploration, 267, 107601. https://doi.org/10.1016/j.gexplo.2024.107601
25. Ran, J., Qiu, X., Hu, Z., Liu, Q., Song, B., & Yao, Y. (2019). Effects of particle size on flotation performance in the separation of copper, gold and lead. Powder Technology, 344, 654–664. https://doi.org/10.1016/j.powtec.2018.12.045
26. Roy, T., Plante, B., Benzaazoua, M., & Demers, I. (2023). Geochemistry and mineralogy of a spodumene- pegmatite lithium ore at various mineral beneficiation stages. Minerals Engineering, 202, 108312. https://doi.org/10.1016/j.mineng.2023.108312
27. Sagzhanov, D., Ito, J., Altansukh, B., Godirilwe, L. L., Haga, K., Takasaki, Y., & Shibayama, A. (2025). Lithium Ore Beneficiation: Sustainable Approaches for Efficient Recovery of Lithium from a Low Grade Spodumene Ore. Journal of Sustainable Metallurgy. https://doi.org/10.1007/s40831-025-01086-3
28. Şen, M., Özcan, M., & Eker, Y. R. (2024). A review on the lithium-ion battery problems used in electric vehicles. Next Sustainability, 3, 100036. https://doi.org/10.1016/j.nxsust.2024.100036
29. Stefan-Henningsen, E., Roberts, N., & Kiani, A. (2025). Enhancing tribological performance: A comprehensive review of graphene-based additives in lubricating greases. Results in Engineering, 25, 104551. https://doi.org/10.1016/j.rineng.2025.104551
30. Semsari Parapari, P., Parian, M., & Rosenkranz, J. (2020). Breakage process of mineral processing comminution machines – An approach to liberation. Advanced Powder Technology, 31(9), 3669–3685. https://doi.org/10.1016/j.apt.2020.08.005
31. Stern, R. J., Ali, K. A., Abdelsalam, M. G., Wilde, S. A., & Zhou, Q. (2012). U–Pb zircon geochronology of the eastern part of the Southern Ethiopian Shield. *Precambrian Research*, *206–207*, 159–167. https://doi.org/10.1016/j.precamres.2012.02.008

32. Tadesse, S. (2001). Geochemistry of the Pegmatitic Rocks and Minerals in the Kenticha Belt, Southern Ethiopia: Implication to Geological Setting. Gondwana Research, 4(1), 97–104. https://doi.org/10.1016/S1342-937X(05)70658-4
33. Tian-ming, G., Na, F., Wu, C., Tao, D., MNR Key Laboratory of Metallogeny and Mineral Assessment, Institute of Mineral Resources Chinese Academy of Geological Sciences, Beijing 100037, China, Research Center for Strategy of Global Mineral Resources, Chinese Geological Survey, Beijing 100037, China, China Huanqiu Contracting & Engineering Corp., LTD Beijing Branch, Beijing 100012, China, & SDU Life Cycle Engineering, Department of Green Technology, University of Southern Denmark, Odense 5230, Denmark. (2023). Lithium extraction from hard rock lithium ores (spodumene, lepidolite, zinnwaldite, petalite): Technology, resources, environment and cost. China Geology, 6(1), 137–153. https://doi.org/10.31035/cg2022088
34. Timich, M., Contessotto, R., & Ulsen, C. (2023). Process Mineralogy of Li-Enriched Pegmatite Combining Laboratory Mineral Separations and SEM-Based Automated Image Analysis. Minerals, 13(3), 343. https://doi.org/10.3390/min13030343
35. Vasilyeva, N., Golyshevskaia, U., & Sniatkova, A. (2023). Modeling and Improving the Efficiency of Crushing Equipment. Symmetry, 15(7), 1343. https://doi.org/10.3390/sym15071343
36. Whitworth, A. J., Forbes, E., Verster, I., Jokovic, V., Awatey, B., & Parbhakar-Fox, A. (2022). Review on advances in mineral processing technologies suitable for critical metal recovery from mining and processing wastes. Cleaner Engineering and Technology, 7, 100451. https://doi.org/10.1016/j .clet.2022.100451
37. Zubi, G., Dufo-López, R., Carvalho, M., & Pasaoglu, G. (2018). The lithium-ion battery: State of the art and future perspectives. Renewable and Sustainable Energy Reviews, 89, 292–308. https://doi.org/10.1016/j.rser.2018.03.002

Appendix. 1

Geochemical AAS analysis result of major and minor oxides of burkuke pegmatite

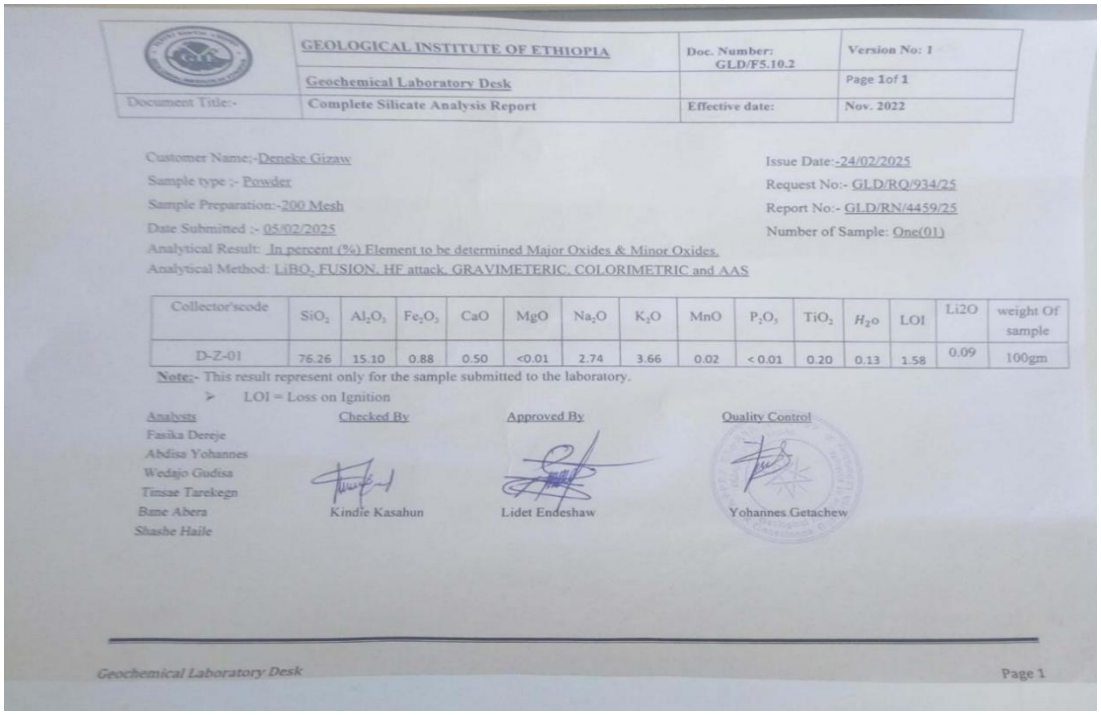

GEOLOGICAL INSTITUTE OF ETHIOPIA	Doc. Number: GLD/F5.10.2	Version No: 1
Geochemical Laboratory Desk		Page 1of 1
Document Title:- Complete Silicate Analysis Report	Effective date:	Nov. 2022

Customer Name:-Deneke Gizaw
Sample type :- Powder
Sample Preparation:-200 Mesh
Date Submitted :- 05/02/2025
Analytical Result: In percent (%) Element to be determined Major Oxides & Minor Oxides.
Analytical Method: $LiBO_2$ FUSION, HF attack, GRAVIMETERIC, COLORIMETRIC and AAS

Issue Date:-24/02/2025
Request No:- GLD/RQ/934/25
Report No:- GLD/RN/4459/25
Number of Sample: One(01)

Collector'scode	SiO_2	Al_2O_3	Fe_2O_3	CaO	MgO	Na_2O	K_2O	MnO	P_2O_5	TiO_2	H_2o	LOI	Li2O	weight Of sample
D-Z-01	76.26	15.10	0.88	0.50	<0.01	2.74	3.66	0.02	< 0.01	0.20	0.13	1.58	0.09	100gm

Note:- This result represent only for the sample submitted to the laboratory.
- LOI = Loss on Ignition

Analysis: Fasika Dereje, Abdisa Yohannes, Wedajo Gudisa, Timsae Tarekegn, Bane Abera, Shashe Haile
Checked By: Kindie Kasahun
Approved By: Lidet Endeshaw
Quality Control: Yohannes Getachew

Geochemical Laboratory Desk Page 1